

QUALIFYING PAPER

For the degree of

bachelor

(degree name)

topic: **Development of a power supply system based on a predictive control
algorithm for autonomous consumers**

Submitted by: fourth year student IEE, group 42

specialty 141 “Electrical Power Engineering, Electrical
Engineering and Electromechanics”

(code and name of specialty)

Kasongo Valerie
Bwanga

(signature)

(surname and initials)

Supervisor

(signature)

Filiuk Ya.O
(surname and initials)

Standards verified by

(signature)

Filiuk Ya.O
(surname and initials)

Head of Department

(signature)

Koval V.P.
(surname and initials)

Reviewer

(signature)

Savkiv V. B.
(surname and initials)

Ministry of Education and Science of Ukraine
Ternopil Ivan Puluj National Technical University

Faculty Applied Information Technologies and Electrical Engineering
(full name of faculty)

Department Department of electrical engineering
(full name of department)

APPROVED BY

Head of Department

(signature) Vadym KOVAL
(surname and initials)

« » 20__

ASSIGNMENT
for QUALIFYING PAPER

for the degree of _____ bachelor _____
(degree name)

specialty 141 "Electrical Power Engineering, Electrical Engineering and Electromechanics"
(code and name of the specialty)

student _____ Kasongo Valerie Bwanga _____
(surname, name, patronymic)

1. Paper topic Development of a power supply system based on a predictive control algorithm for autonomous consumers

Paper supervisor Filiuk Yaroslav Oleksandrovych, Ph.D.
(surname, name, patronymic, scientific degree, academic rank)

Approved by university order as of «05» 02 2024 № 4/7-110

2. Student's paper submission deadline 20.08.2024 _____

3. Initial data for the paper _____

To conduct a study of the modes of operation of a semiconductor three-phase SES based on a semiconductor converter (inverter) that implements a predictive control algorithm.

4. Paper contents (list of issues to be developed)

1. Analytical section

2. Design and development section

3. Calculation section

4. Safety of life and basics of labour protection

5. List of graphic material (with exact number of required drawings, slides)

1. Title

2. Introduction

3. Model of solar power plant. 4-7 results of solar power plant simulation

4-7 results of solar power plant simulation

8-12 static operation mode of SPS

13 dynamic mode of work of SPS

14-18 experimental results of simulations

19 Conclusions

ESSAY

Bachelor's qualification work. Ternopil Ivan Pulyuy National Technical University. Faculty of Applied Information Technologies and Electrical Engineering. Department of Electrical Engineering, IEE-42 Group. - T.: TNTU, 2024.

Page 54; Fig. 50; Table 6; Drawings; Sources 16; Annexes -.

The topic of the bachelor's qualification work is " Development of a power supply system based on a predictive control algorithm for autonomous consumers".

The purpose of the qualification work is to ensure the necessary quality of the output voltage of an autonomous power supply system based on control algorithms

The conducted studies show that the model predictive voltage control algorithm (MPVC) is effective when applied to three-phase power supply systems implemented on the basis of a semiconductor converter (inverter). To verify the theoretical propositions formulated in this work:

- 1) the MPVC algorithm was refined for use in emergency operation modes of the SPS;
- 2) a mock-up sample of a semiconductor SPS with a zero wire was made, on which physical experiments were carried out;
- 3) as a result of the conducted experiments, it is shown that the parameters of the SPS output voltage according to the THD and dynamic response indicators correspond to the results obtained during simulation modeling.

Key words: solar energy, controller, computer simulation.

ESSAY	3
CONTENT	4
Introduction	6
1 Analytical section	8
1.1 Micro Grid as a Small Distributed Energy Concept	8
1.1.1. Micro Grid DC	8
1.1.2. Micro Grid AC	9
1.1.3. Hybrid Micro Grid	10
1.2 Structures of semiconductor converters in SPS	11
1.2.1 Two-stage conversion systems	11
1.2.1. Single-stage conversion systems	12
1.3 Topologies of three-phase AIVs in SPS	13
1.3.1. Simple topology of three-phase AIV	13
1.3.2 Topology of three-phase AIV with the middle point of the capacitor in the power circuit	14
1.3.3 Topology of three-phase AIV with zero wire	15
1.3.4 Topology based on three separate single-phase inverters	15
1.4 Appendix to the section	17
2 Design and development section	18
2.1 Comparative analysis of SPS control algorithms	18
2.2 Selection of linear control algorithm	20
2.3 Static mode of operation of SPS	24
2.4 Dynamic mode of operation of the SPS	28
2.5 Control sensitivity analysis	29
2.6 Conclusions to the section	31
3 Calculation section	32
3.1 Optimisation of the MPVC algorithm	33
3.2 Experimental results of simulations carried out	34
3.2.1 Static mode	37
3.2.2 Dynamic mode	42
3.2.3 Emergency mode	43

3.3 Conclusions to the section	46
4 Safety of life and basics of labour protection	47
4.1 Safety in the operation of electrical equipment and power grids	47
4.2 Study of the sustainability of work in emergencies of enterpriSPS of the electrical and lighting industry	49
General conclusions	52
List of links	53

INTRODUCTION

Relevance of work. To date, it can be stated that the world energy system has entered a new stage of fundamental transformation. In general, this set of changes is called the "Energy Transition", formed under the influence of changes in energy policy and the development of new technologies, which involves the wide use of renewable energy sources when displacing fossil fuels.

Renewable energy sources combined in microgrids (microgrids) can be a cost-effective way to provide access to reliable and inexpensive energy supply to those who now live without electricity, and such solar power systems (SPS) can operate both autonomously and together with the main electrical networks.

Autonomous SPS, as a rule, operate in conditions of limiting the power of the input source, as well as the "unpredictability" of loads, which determines their random nature, both in terms of active power and by nature - loads can be single- or three-phase, balanced (symmetrical) or unbalanced, linear or non-linear. Asymmetry and harmonic voltage distortions can cause serious equipment problems such as vibration, overvoltage, overheating, etc.

Autonomous power supply systems usually consist of a power source, loads, power electronic devices and energy storage systems. An autonomous SPS behaves like a controlled object.

The main power electronic devices in SPS are inverters, which are used as interfaces for connecting a power source to AC loads. The main function of inverters is power transmission and control. In addition, by proper control of inverters, voltage imbalance problems can be solved, as well as compensation for higher harmonics.

With the high prevalence of semiconductor SPS in the energy sector of industrial and autonomous objects, the use of new circuitry and algorithmic solutions that allow to improve the quality of their work is an urgent task.

The purpose of the work is to ensure the necessary quality of the output voltage of an autonomous power supply system based on control algorithms.

To achieve this goal, it is necessary to solve the following tasks:

To study and analyse the features of the application and construction of autonomous semiconductor SPS when working on different types of loads and as part of autonomous networks, in particular, microgrid.

Conduct comparative studies of SPS with predictive control of SPS, functioning on the basis of algorithms of proportional-integral-differential (PID) and proportional-resonance (PR)-regulation.

Develop algorithms for emergency protection of semiconductor SPS with predictive load current control.

In confirmation of theoretical studies, conduct an experimental check of predictive control algorithms.

1. ANALYTICAL SECTION

1.1 Micro Grid as a concept of small distributed energy.

The concept of Micro Grid involves the creation in certain territories of a potentially autonomous energy network structure containing its own sources of electricity and capable of solving the problem of supplying consumers both independently (autonomously) and at maximum peak loads, when the central network is not able to provide the consumer with high-quality electricity. The Micro Grid concept also involves the use of renewable energy sources, which every year, due to the deteriorating environmental situation, are becoming more and more in demand. It is the use of renewable sources that allows you to solve the task of energy efficiency of SPS.

Micro Grid includes a set of generating power sources. Generating sources can be represented by a combination of traditional sources powered by diesel fuel (diesel generators) or gas (gas piston engines), small hydroelectric power plants, as well as wind turbines and solar stations.

There is no definite power limit for Micro Grid. For example, ABB has set itself a border with a capacity of about 20 MW. There is also the NanoGrid concept, whose networks are characterised by capacities up to 50 kW. The use of advanced technologies in the field of power electronics, microprocessor technology and electrical material science is decisive in the concept of Micro Grid (NanoGrid). In this sense, Micro Grid can include DC or AC power transmission devices, it is possible to use frequency-controlled electric drives, effective low-cost power transformers, illuminators on LED technologies, etc. The central power converting device of Micro Grid is an autonomous inverter voltage - AIV (current - AIC) as a link,

Classification of Micro Grid SPS configurations can be performed according to the method used for power transmission and distribution [11]. This classification consists of Micro Grid DC, Micro Grid AC and hybrid Micro Grid.

1.1.1. Micro Grid DC

DC microgrids are widely used in telecommunication systems, electric vehicles, etc. In addition, the intensive use of electronic loads in office buildings and commercial facilities and the rapid growth of DC power sources such as photovoltaic and fuel cells

make DC microgrids an attractive network solution. In Fig. 1.1 depicts the typical structure of a DC microgrid based on power electronics devices - DC-DC converters, rectifiers and autonomous voltage inverters.

A controller that monitors (with the formation of the necessary commands) for load consumption modes and individual converters, the charge of the battery from the PMSG synchronous wind turbine or from the PV solar panel, the blocking of SPS emergency modes is not conditionally shown.

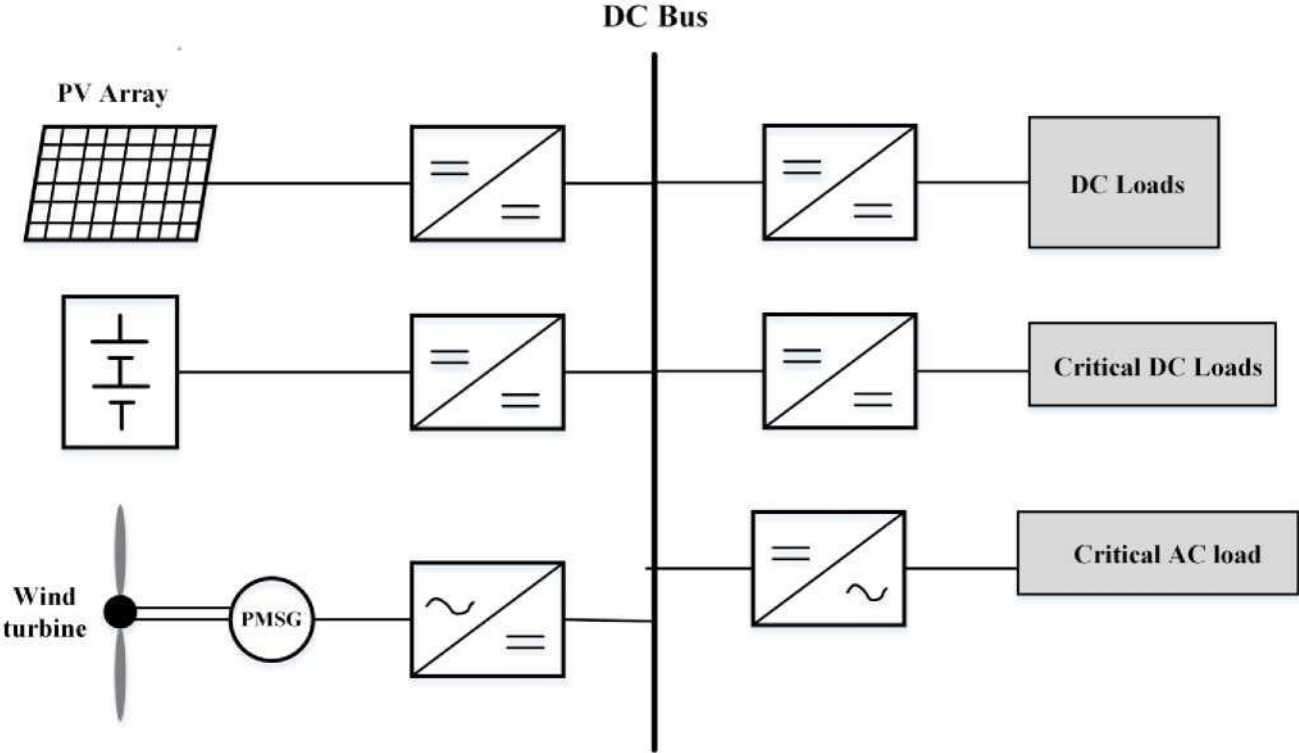


Figure 1.1. Structure of the DC Micro Grid

1.1.2. Micro Grid AC

In Fig. 1.2 shows a typical configuration of AC microgrids based on power electronics devices. In this configuration, power supplies are directly connected to the AC bus and load through separate converters [12] in one or two stages, as will be discussed in the next section. If any of the converters fails due to lack of electricity in the channel, the microgrid can provide the necessary amount of energy from the remaining sources [13]. However, this system has a disadvantage in expensive investments and requires a complex control algorithm for converters to regulate power, voltage (current) formed in a common AC bus. So, for example, a system of rigid synchronisation of autonomous voltage inverters in phase and the magnitude of instant voltages is required.

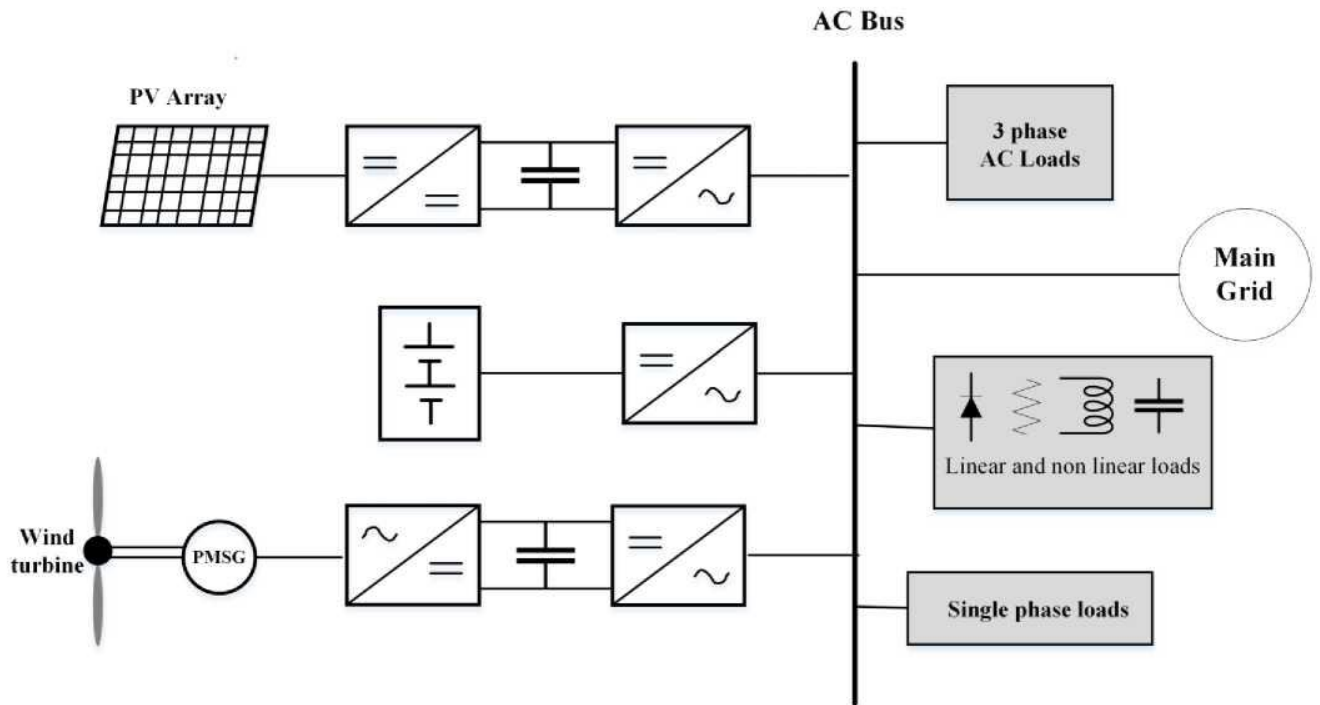


Figure 1.2. Structure of the AC Micro Grid

1.1.3. Hybrid Micro Grid

In hybrid microgrids [14, 15], the common DC bus collects adjustable power from various power sources, provides DC load and maintains a constant DC voltage at the input terminal of an autonomous voltage inverter. The inverter is used to connect a common DC bus to AC loads, as shown in Fig. 1.3. A controller that monitors (with the formation of the necessary commands) for load consumption modes and individual converters, the charge of the battery from the PMSG synchronous wind turbine or from the PV solar panel, the blocking of SPS emergency modes is not conditionally shown. Unlike the previous scheme for an autonomous inverter, designed in this case for full load power,

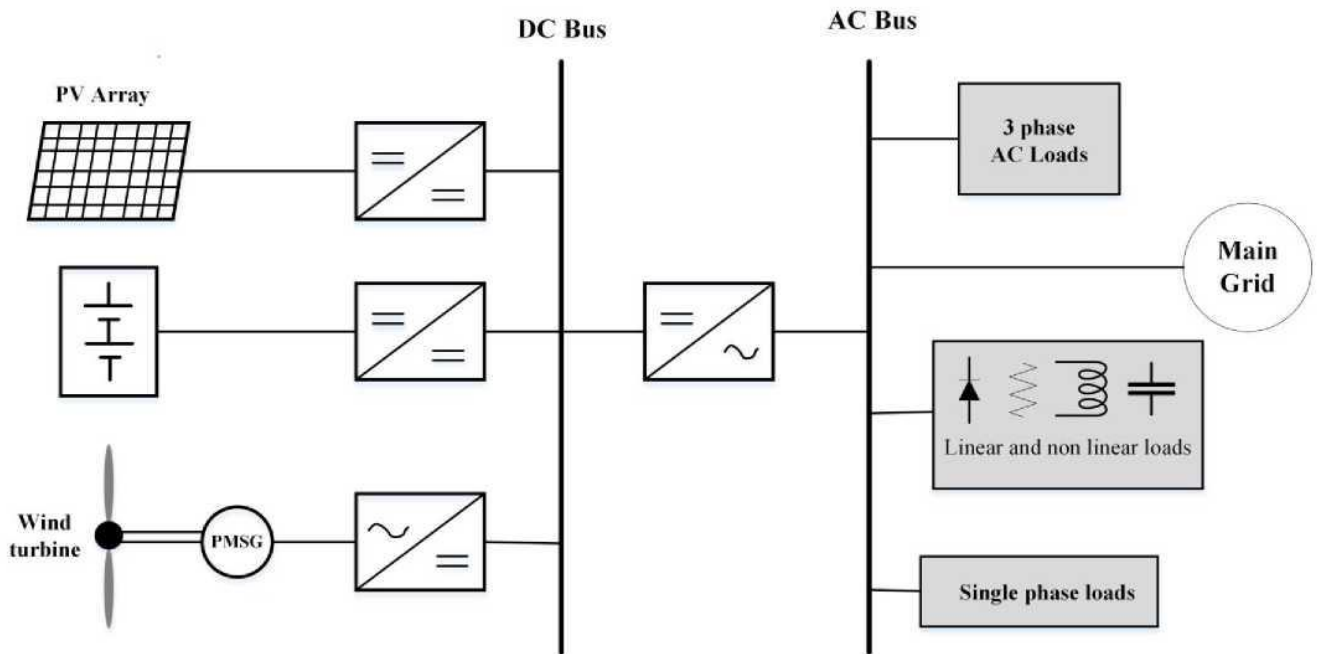


Figure 1.3. Structure of the hybrid Micro Grid

1.2 Structures of semiconductor converters in SPS

The structures of power source connections in SPS are determined by the types of primary energy resources, load requirements and microgrid structures [16]. The topology of semiconductor converters can be divided into two categories depending on the number of energy conversion stages.

1.2.1 Two-stage conversion systems

A two-stage energy conversion system is the most common configuration for power supplies. In Fig. 1.4 shows two typical structures of a two-stage conversion system for photovoltaic systems and wind turbines, respectively. In general, a two-stage conversion system consists of the first stage of a DC converter with DC output voltage or a rectifier for these energy sources with AC output voltage, the second stage is an inverter for AC load or a DC converter for DC load. This configuration has two separate control systems: the control of the first stage aims to remove the maximum power from the primary power source; the control system of the second stage provides a high-quality conversion of constant voltage variable with the necessary amplitude, frequency, coefficient of harmonious distortion in the conditions of the nature of a given load.

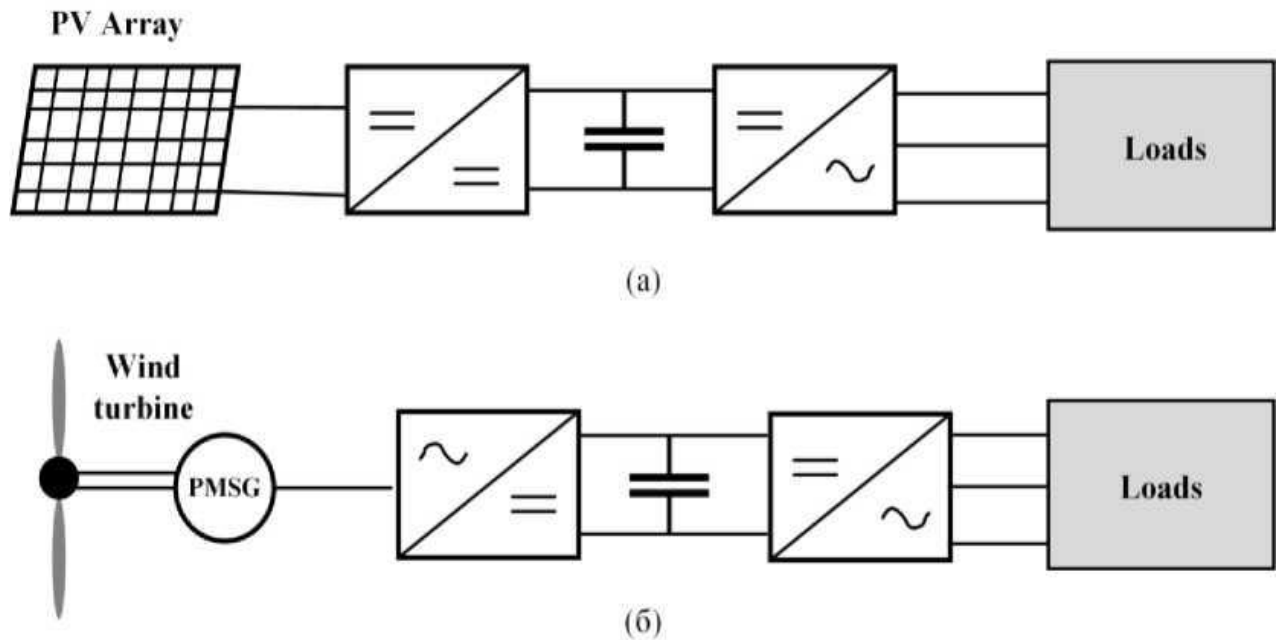


Figure 1.4. Two structures of two-stage conversion systems (a) for photovoltaic system (b) for wind turbine system

1.2.2 Single-stage conversion systems

In Fig. 1.5 shows the basic configuration of a single-stage conversion system for power supplies that create DC voltage. This configuration provides the advantages of high efficiency, small size and weight, as well as cost reduction. However, this requires a complex control system to perform the function of a two-stage configuration: as in the previous example, the control system must provide high-quality conversion of constant voltage to variable with the required amplitude, frequency, coefficient of harmonic distortion in conditions of the nature of a given load, as well as maximum power selection from the PV solar panel.

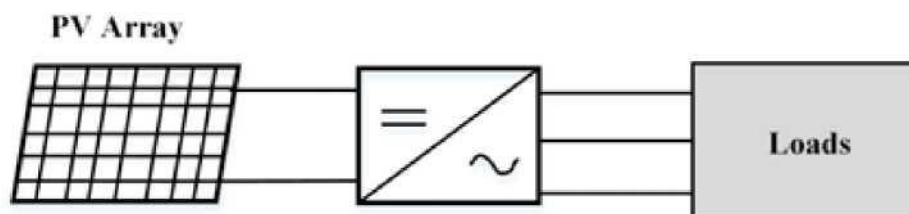


Figure 1.5. Structure of a single-stage conversion system for photovoltaic system

1.3 Topologies of three-phase AIVs in SPS

1.3.1. Simple topology of three-phase AIV

In Fig. 1.6 depicts a three-conductored topology of a three-phase AIV with an output filter [17]. The operation of AIV keys is assumed as a latitudinal pulse modulation of the output voltage followed by the filtration of higher harmonics in the output LC filter. The main feature of such a topology is the inability of its operation on a non-symmetrical, and, even more so, non-linear load, firstly, due to the absence of a fourth (zero) wire, and, secondly, the great complexity of organising a control system to reduce inconvenience from this disadvantage. Alternatively, you can use this topology, but with an L-Y transformer [18,19] or a zigzag transformer [20], which is heavy and expensive and therefore undesirable in many applications

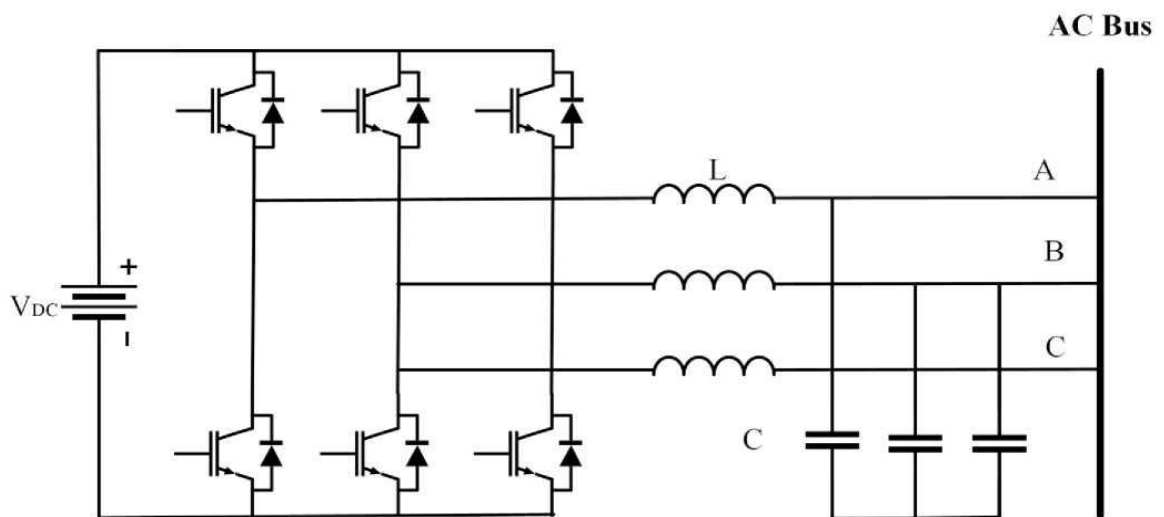


Figure 1.6. Three-phase AIV topology with input filter

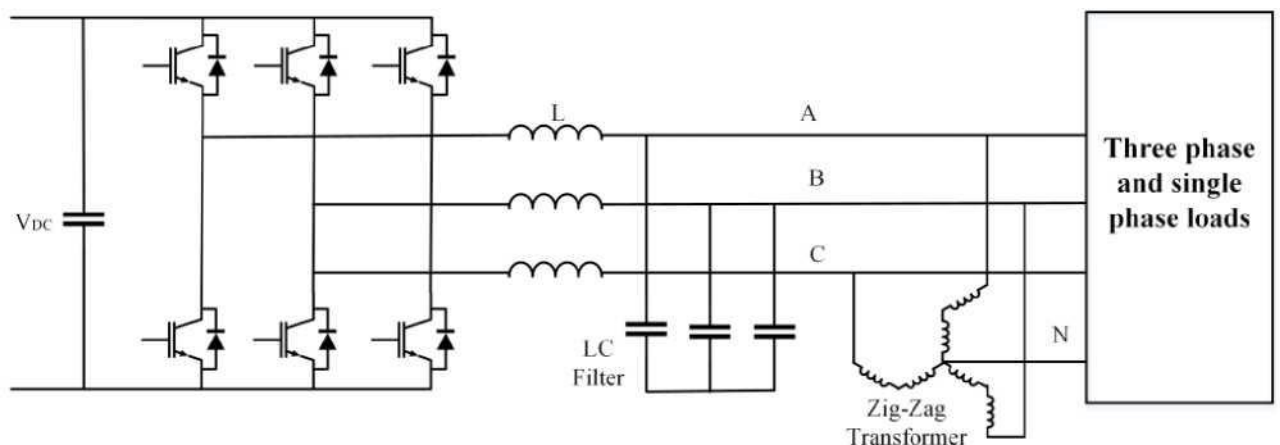


Figure 1.7. Topology of three-phase AIV with a "zigzag" transformer

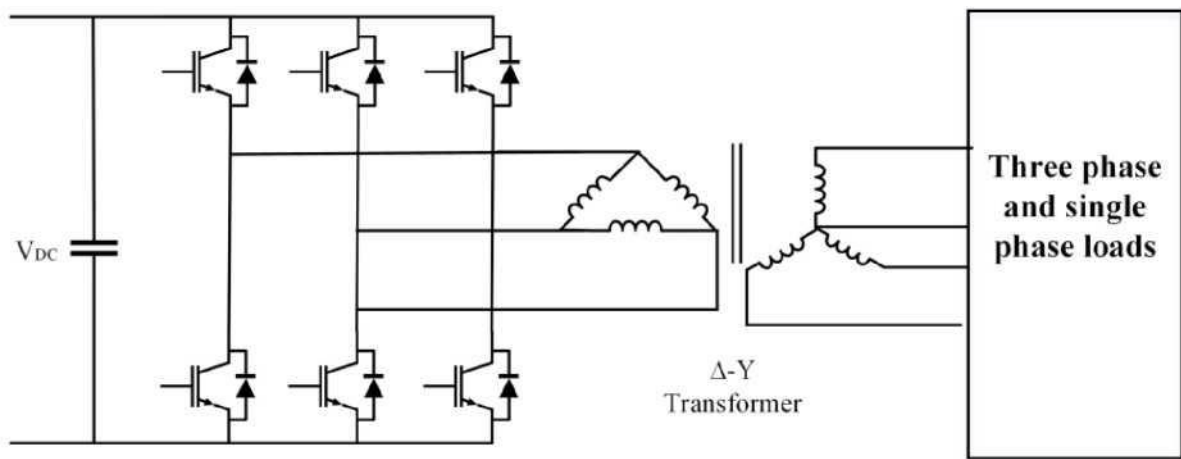


Figure 1.8. Topology of three-phase AIV with ΔY transformer

1.3.2 Topology of three-phase AIV with the middle point of the capacitor in the power circuit

Topology with the midpoint of the capacitor in the power circuit is shown in Fig. 1.9, is the simplest AIV topology with zero wire and with the least number of keys. In this topology, the zero wire is connected to the midpoint of the separated DC capacitors. Fundamentally, this topology can be modelled as three independent single-phase half-bridge inverters. The maximum achievable peak value of the phase voltage at the AIV output in this case is half of the DC bus supply voltage ($V_{dc}/2$). Thus, in order to get 220 per phase, a large DC bus voltage (usually 700 V) is required. This circuit requires expensive and large capacitors to achieve an equal distribution of voltage between split capacitors [20].

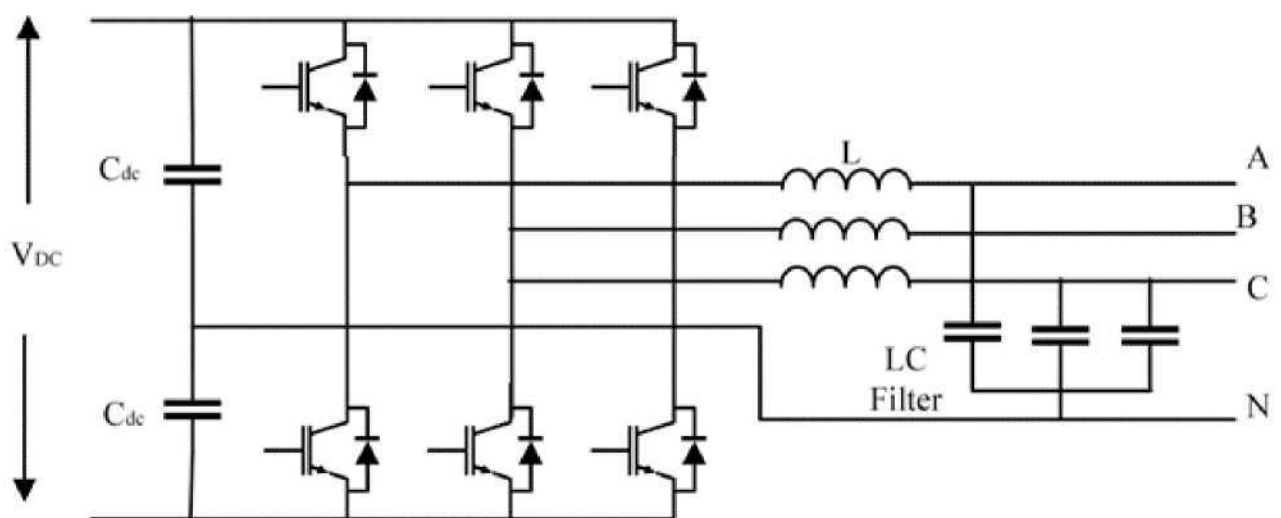


Figure 1.9. Topology with the centre point of the capacitor

1.3.3 Topology of three-phase AIV with zero wire

Among SPS developers, there is growing interest in the use of three-phase inverters with zero wire due to their ability to effectively handle unbalanced loads in four-wire autonomous systems. In this topology, the neutral wire is connected to an artificially created midpoint in the fourth rack (Figure 1.10). DC bus capacitors are only used to eliminate pulsation on the DC bus (the midpoint of the DC bus is not used, so there is no problem of capacitor voltage imbalance in this converter). Thus, the capacitors used, DC buSPS are relatively small. The maximum achievable peak value of the output phase voltage is higher than the AIV value with the mean point of the capacitor (compared to $0.5 V_{dc}$). Therefore, the voltage level requirement of the DC bus becomes lower, and switching loss decreases, which leads to increased efficiency. The presence of two additional transistor keys leads to the complication of the control algorithm, which in principle can be taken into account the modern level of development of microprocessor technology.

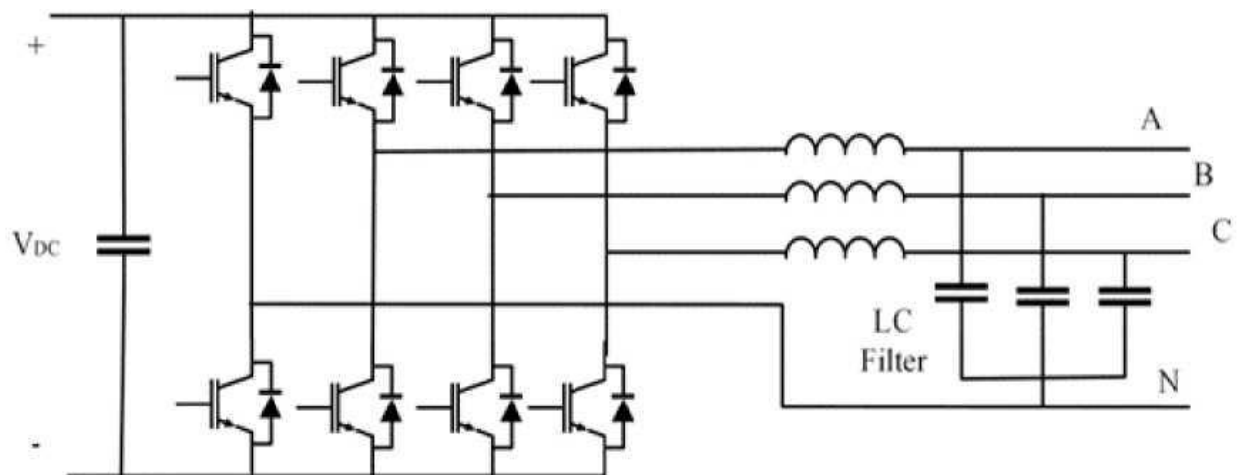


Figure 1.10. Topology of three-phase AIV with zero wire

1.3.4 Topology based on three separate single-phase inverters

This type of converter consists of three single-phase inverters that are connected to loads through a dividing transformer, as shown in Figure 1.11. Compared to other topologies, this topology has advantages such as a low DC voltage requirement for a given output voltage, which is half that of an inverter with a midpoint of the capacitor.

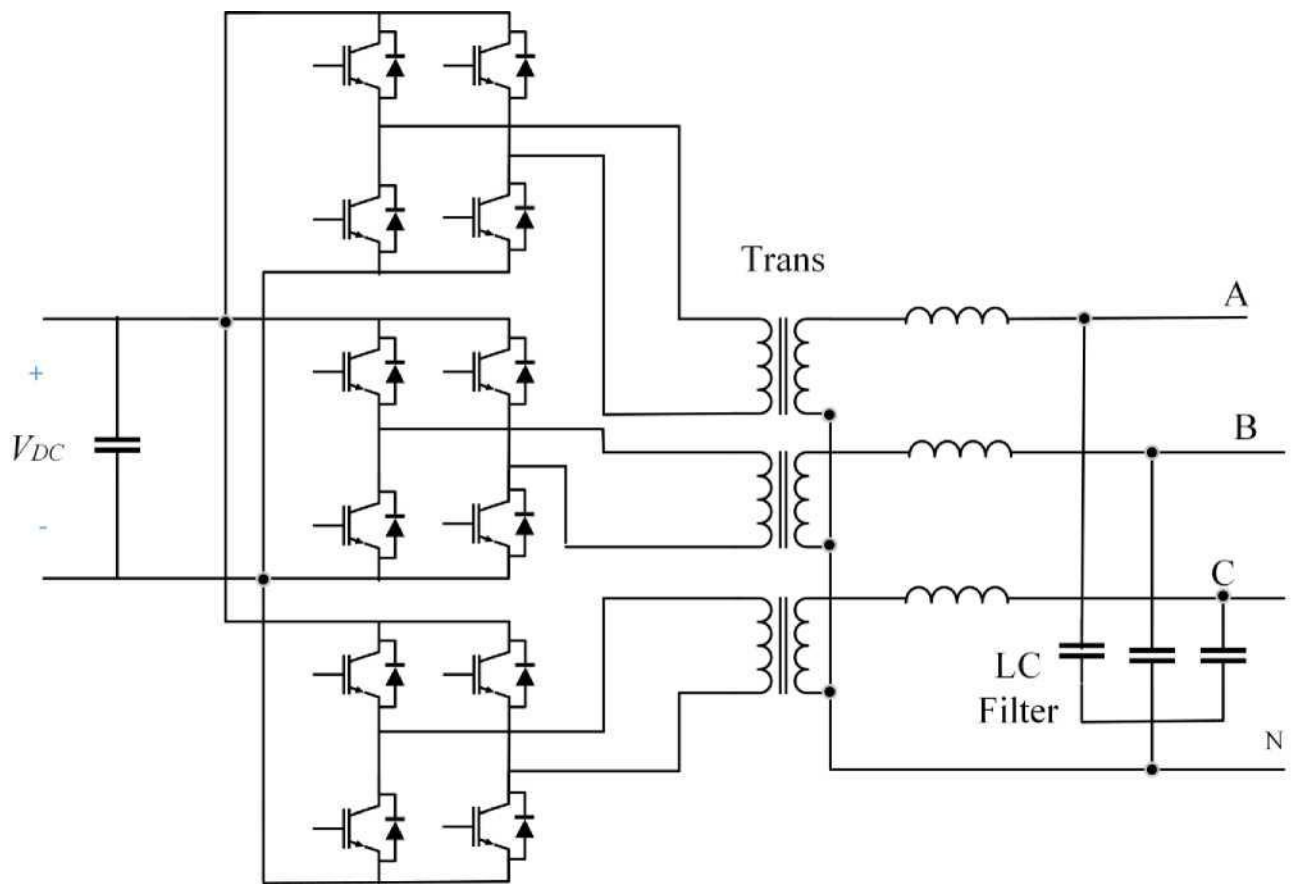


Figure 1.11. SEM topology based on three separate single-phase inverters

Although more transistors are required in this topology, the output voltage has the best harmonic profile, and the requirement for output passive filters decreases. Higher reliability can be achieved here, because each phase is independent and during a failure in any phase, the other two phases can still provide three-phase loads. Thus, the scheme allows phase-by-phase adjustment of the output voltage. The main disadvantage of this topology is the need to use separation transformers operating at the main frequency, which are necessary for insulation, safety and voltage matching. In this sense, the lack of "agreement" can turn into dignity if, for example, SPS is used in the purpose of an uninterruptible power supply source, when the DC link is represented by a battery. In this case, it is advisable to perform a smoothing filter with the placement of the throttle in the primary low-voltage circuit, and the filter capacitor in the output of the high-voltage circuit, the throttle energy is determined by its current, and the capacitor energy is by voltage (Figure 1.12).

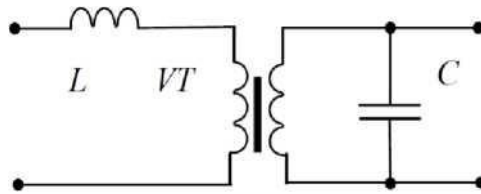


Figure 1.12: A variant of the smoothing filter

1.4 Appendix to the section

Micro Grid as a concept of small distributed energy was analysed. The configuration of semiconductor autonomous SPS is considered. A review analysis of methods for controlling technical systems capable of finding application in autonomous semiconductor SPS was carried out.

2. DESIGN AND DEVELOPMENT SECTION

2.1 Comparative analysis of SPS control algorithms

Based on the analysed topological schemes and mathematical models, the Matlab Simulink package developed appropriate simulation models (see fig. 2.1-2.4) SPS parameters and loads used in modelling are given in tables 2.1, 2.2. Modelling of SPS operation with zero wire was carried out in order to compare the quality of output voltage formation in static and dynamic modes, as well as to study the sensitivity of control to load changes and parameters of the output LC filter. At the same time, balanced (symmetrical) and unbalanced (asymmetrical) active and actively inductive loads were used, as well as nonlinear loads (symmetrical and asymmetrical).

Table 2.1 SPS modelling parameters

Parameter	Value
DC link voltage of the AIV	V _{dc} = 640 V
Sampling time	T _s =20 μs
PWM switching frequency	f _s =4000 Hz
Capacitance of the DC capacitor	C _{dc} =1000 μF
LC filter parameters	L = 2.5 mH, C = 80 μF

Table 2.2 SPS load parameters

Experiment	Load parameters
1) Balanced resistive loads	R _a = R _b = R _c = 15
2) Balanced inductive loads	R _a = R _b = R _c = 10 Ω, L _a = L _b = L _c = 20 mH
3) Unbalanced resistive loads	R _a = 5 Ω, R _b = 10 Ω, R _c = yes
4) Unbalanced inductive loads	R _a = 5Ω, R _b = 10Ω, R _c = yes L _a = 10mH, L _b = 30mH
5) Unbalanced nonlinear loads	L _a ' = 50 mH, R _a = 20 Ω, R _{b1} '=1 Ω, R _{b2} '=60 Ω, C _b ' = 3000 μF, L _c ' = 20 mH, R _c = 70 Ω, C _c '= 5000 μF

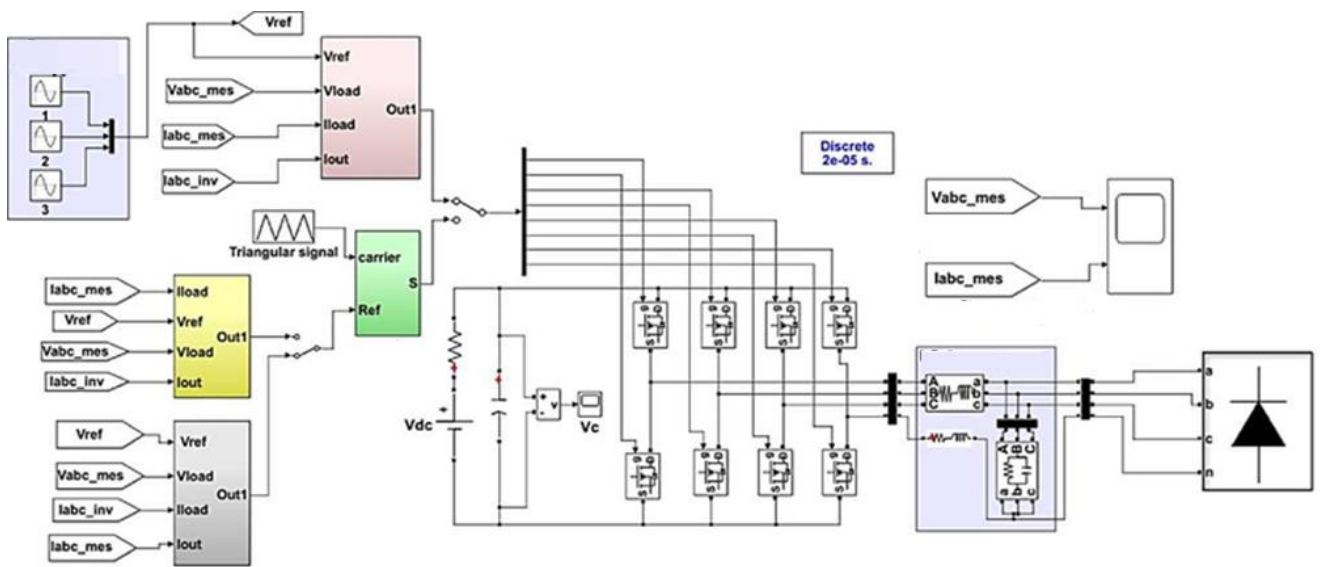


Figure 2.1. Virtual SPS scheme when controlling AIV based on three control methods (MPVC, PR regulator and PID controller)

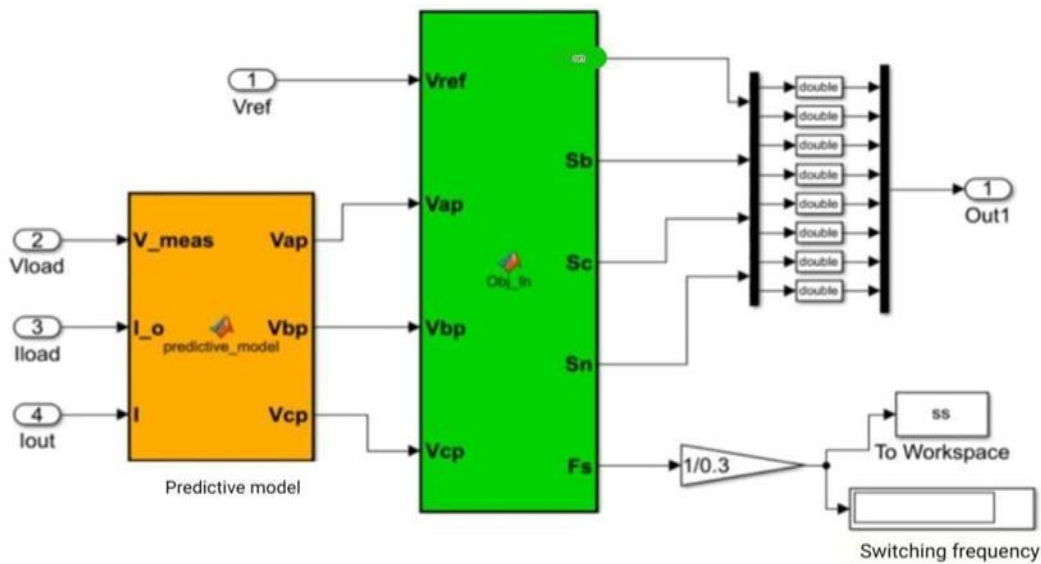


Figure 2.2. Diagram of the model a predictive with control (MPVC) in the Matlab Simulink package.

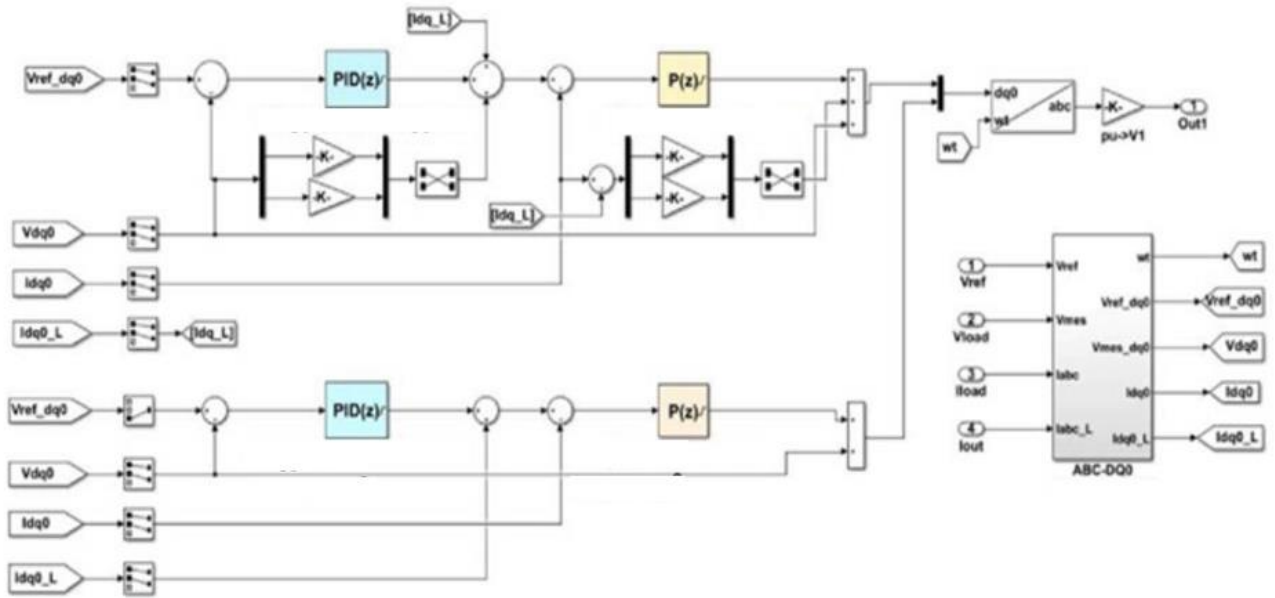


Figure 2.3. Diagram of PID control in the Matlab Simulink package.

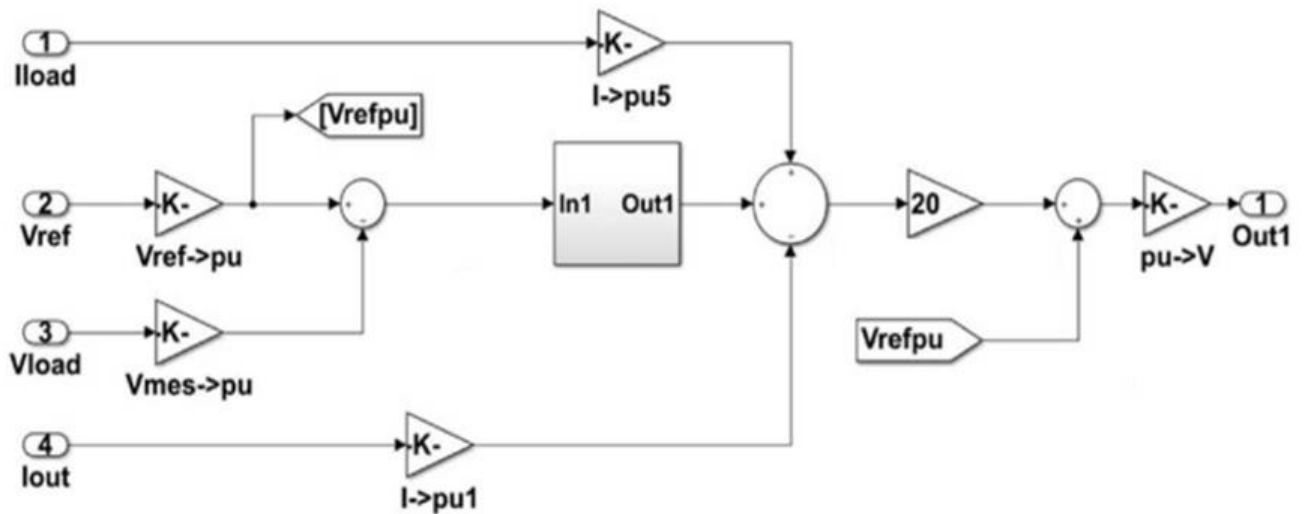


Figure 2.4. PR adjustment diagram in the Matlab Simulink package

2.2 Selection of a Linear Control Algorithm

In the second section, two linear control methods were presented and developed: PID control and PR control, which are based on PWM when adjusting the inverter voltage. In this section, one of these control methods will be selected to perform a comparative analysis with the MPVC.

To identify the effectiveness and stability of these two control methods, three case studies were conducted:

1. Unbalanced resistive loads;
2. Unbalanced inductive loads;

3. Unbalanced nonlinear loads, the topology of which is shown in Figure 2.9.

The load voltage, load currents, and DC link voltage signals for AIV under three load conditions are presented in Figures 2.5-2.7. The results show that both PR and PID controllers are capable of regulating the load voltage with low harmonic distortion for unbalanced resistive and inductive loads.

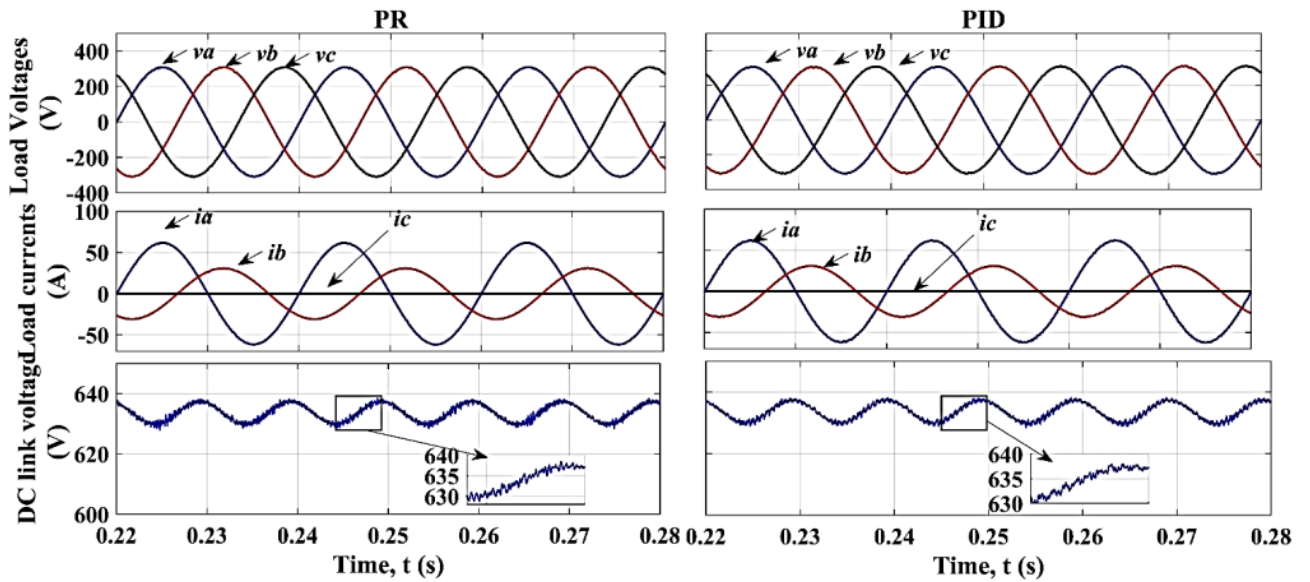


Figure 2.5. Simulation results of the SPS (unbalanced resistive loads) using (a) PR and (b) PID algorithms.

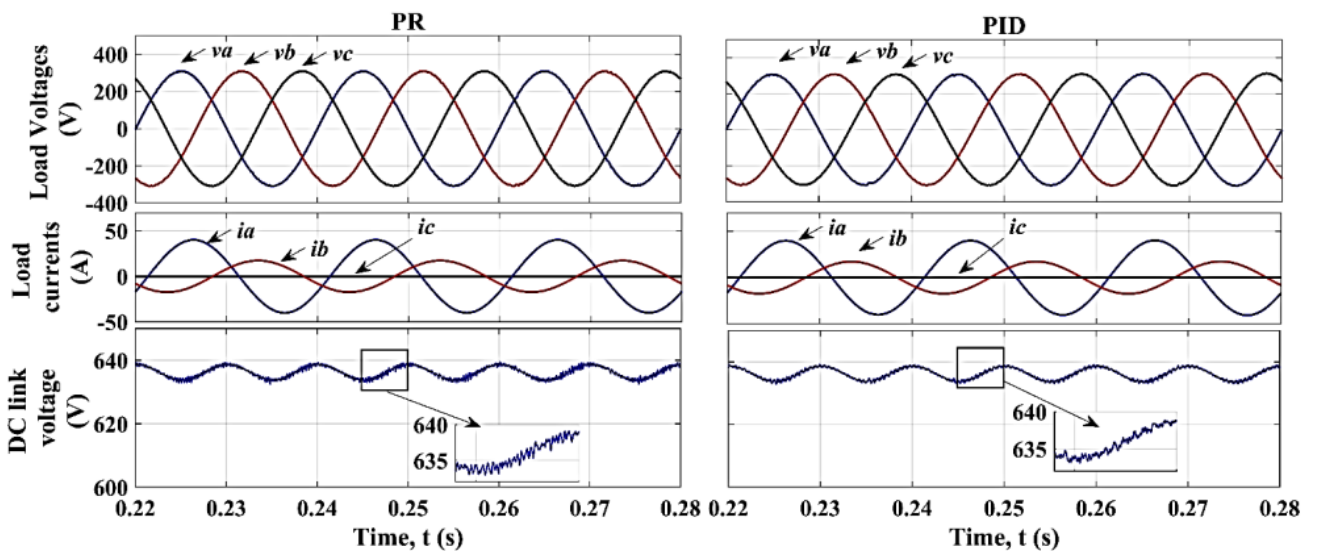


Figure 2.6. Simulation results of the SPS (unbalanced inductive loads) using (a) PR and (b) PID algorithms.

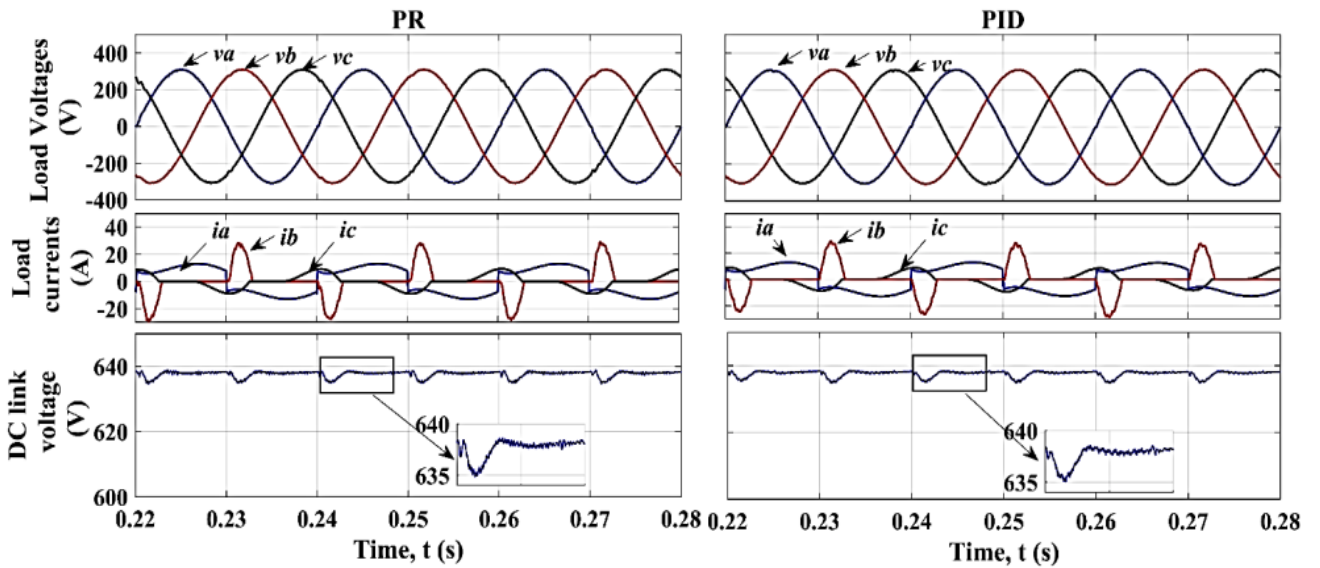


Figure 2.7. Results of SPS modeling (unbalanced nonlinear loads) with (a) PR and (b) PID algorithms

The studies show that, compared to the PID controller, the PR controller provides slightly higher harmonics in the loads, because the PR controller used in this work is based on only one resonant filter for the fundamental frequency. To improve the performance of this control method, more resonant filters of other harmonic frequencies must be added. This makes the control system design very complex. Also, the PI controller provides a higher voltage ripple ($\%V_c$) in the DC link of the AIV compared to the PID controller, but this difference is very small, as shown in Table 2.3.

In the dynamic mode, a step change from no-load to a balanced resistive load ($R_a = R_b = R_c = 10 \Omega$) was applied in 0.2 seconds, the load voltages and currents for the PR and PID algorithms are shown in Fig. 2.8, which additionally shows an enlarged view of the measured voltage with its reference time waveform during this change. Results.

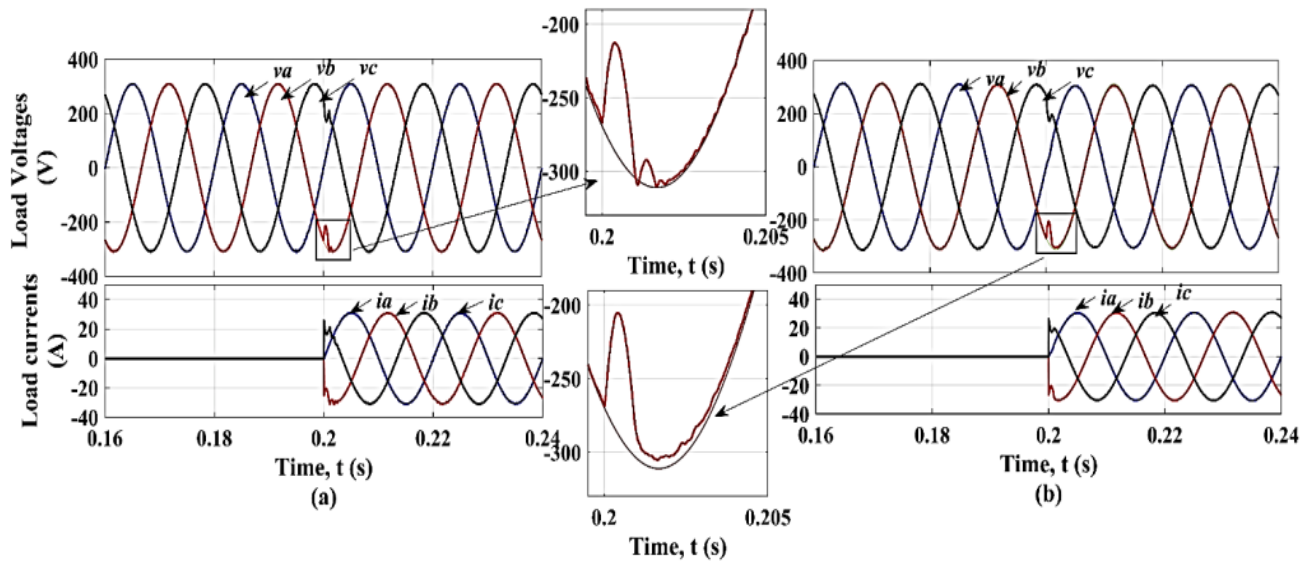


Figure 2.8. SPS load voltages and currents in dynamic mode for (a) PR and (b) PID algorithms

Table 2.3 Comparison of the quality of two linear control methods

Experiments.	PR			PID				
	% ΔV_{dc}	% THD			% ΔV_{dc}	% THD		
		Φ_a	Φ_b	Φ_c		Φ_a	Φ_b	Φ_c
1) Unbalanced resistive loads	1.65	1.36	1.36	1.46	1.5411	1.45	1.47	1.44
2) Unbalanced inductive loads	1.084	1.55	1.56	1.53	1.0109	1.49	1.48	1.45
3) Unbalanced nonlinear loads	0.818	1.72	1.66	1.65	0.7095	1.62	1.5	1.54

Among the presented results, the author chose a PID controller as the linear controller for further use in a comparative study with MPVC because the PID controller is simpler than a PR controller and easier to set its parameters. Additionally, the author found that the PID controller has comparable performance to the PR controller. The following section will conduct a comprehensive comparative study of the proposed MPVC algorithm and the presented PID regulation.

2.3 Static Mode of SPS Operation

Five case studies were conducted to identify the differences between MPVC and PID in static mode. The symmetric and asymmetric three-phase loads can be resistive or inductive and are connected to an inverter. Additionally, single-phase nonlinear loads are used to display the characteristics of the control systems under nonlinear conditions. The topology of these loads is shown in Figure 2.9. The load parameters used in the modeling are given in Table 2.2.

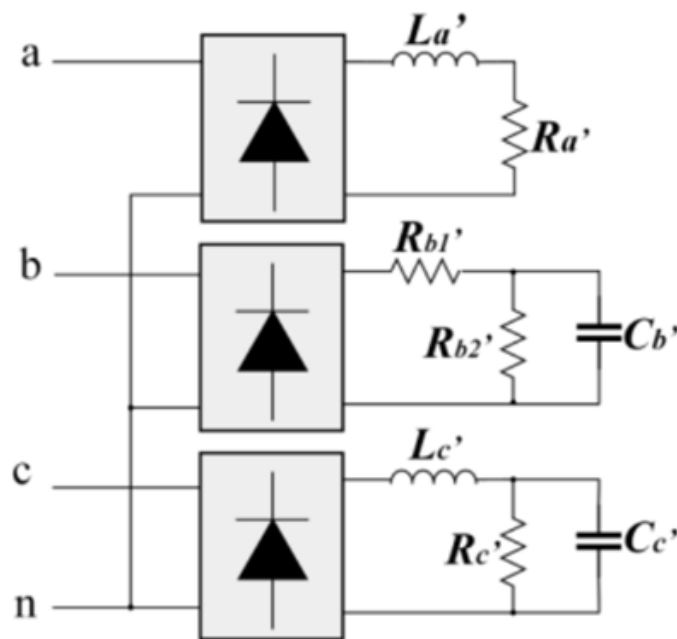


Figure 2.9. Topology of the single-phase SPS loads used in the modeling

The load voltage, load currents, and DC link voltage signals for AIV under five load conditions are presented in Figures 2.10-2.14. To estimate the difference between the MPVC and PID indicators, the switching frequency, total harmonic distortion (THD), Voltage Imbalance Factor (VIF) [18], and voltage ripple (% V_c) are analyzed.

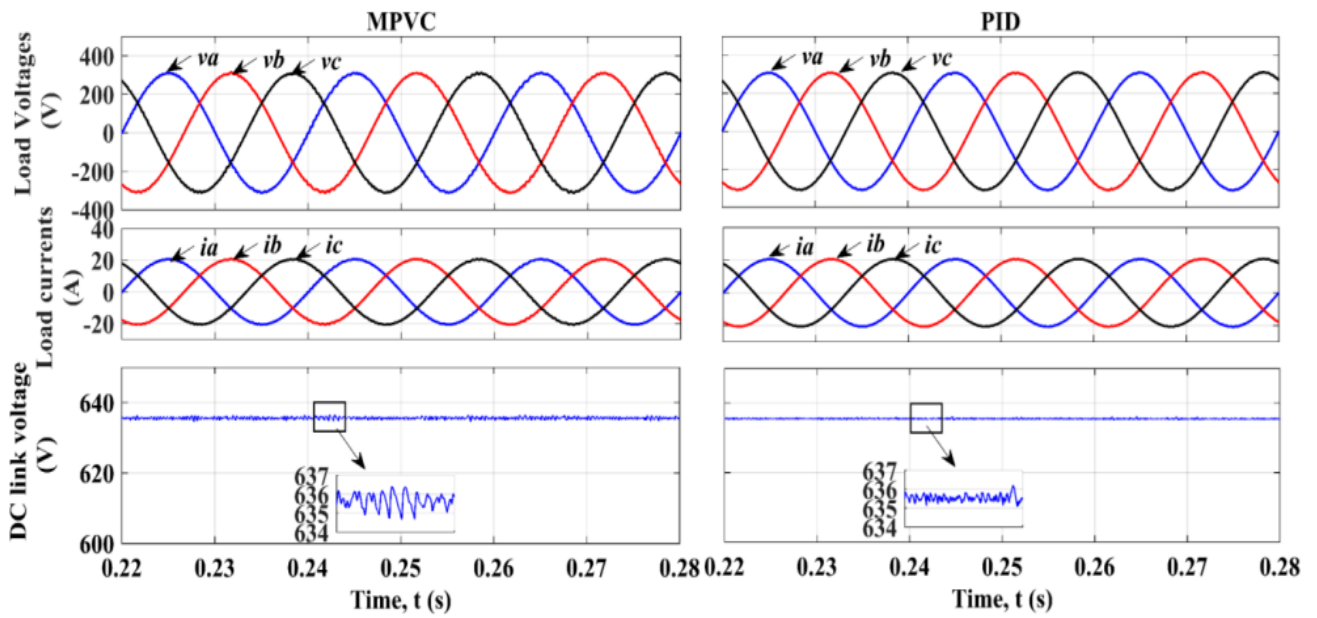


Figure 2.10. Simulation results of the SPS (Case Study 1: Balanced Resistive Loads) using (a) MPVC and (b) PID

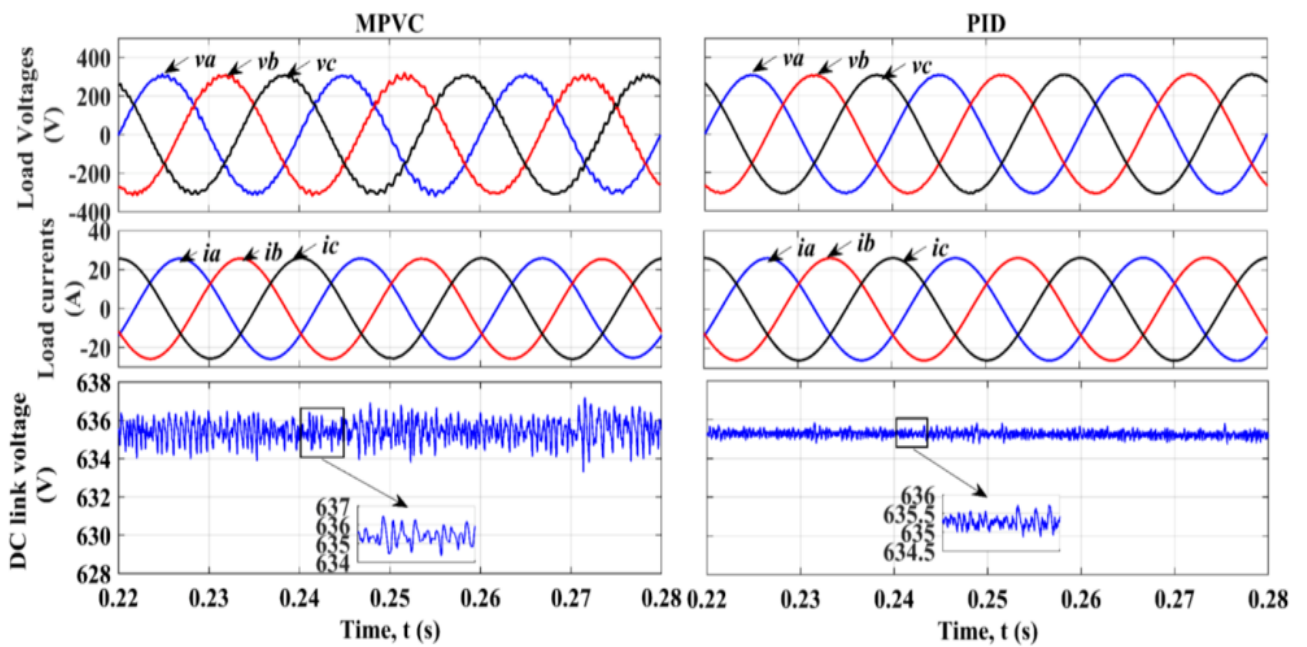


Figure 2.11: Simulation results of the SPS (Case Study 2: balanced inductive loads) using (a) MPVC and (b) PID

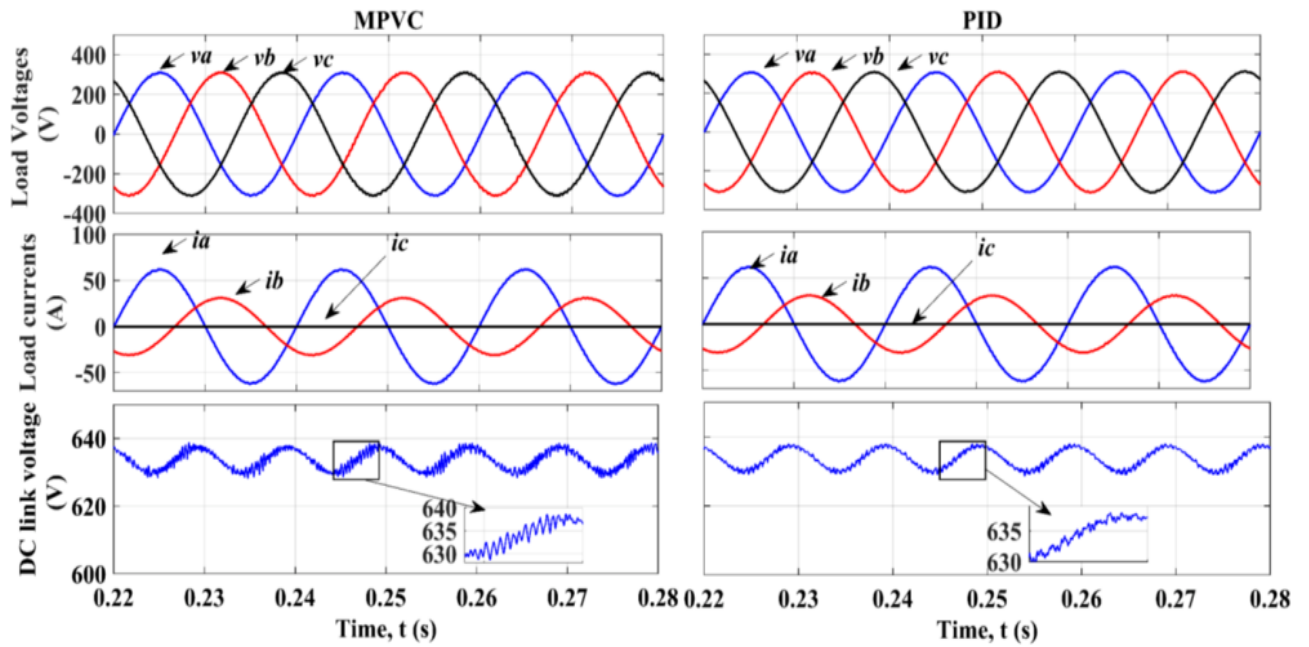


Figure 2.12. Simulation results of the SPS (Case Study 3: Unbalanced Resistive Loads) using (a) MPVC and (b) PID

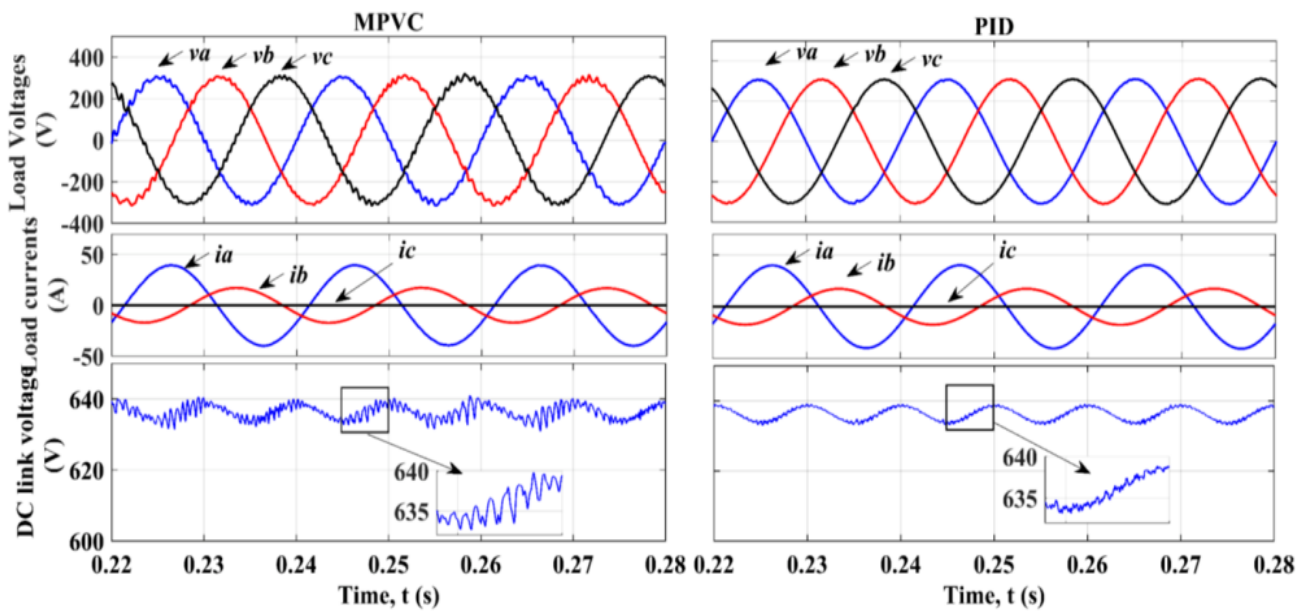


Figure 2.13. Simulation results of the SPS (Case Study 4: unbalanced inductive loads) using (a) MPVC and (b) PID

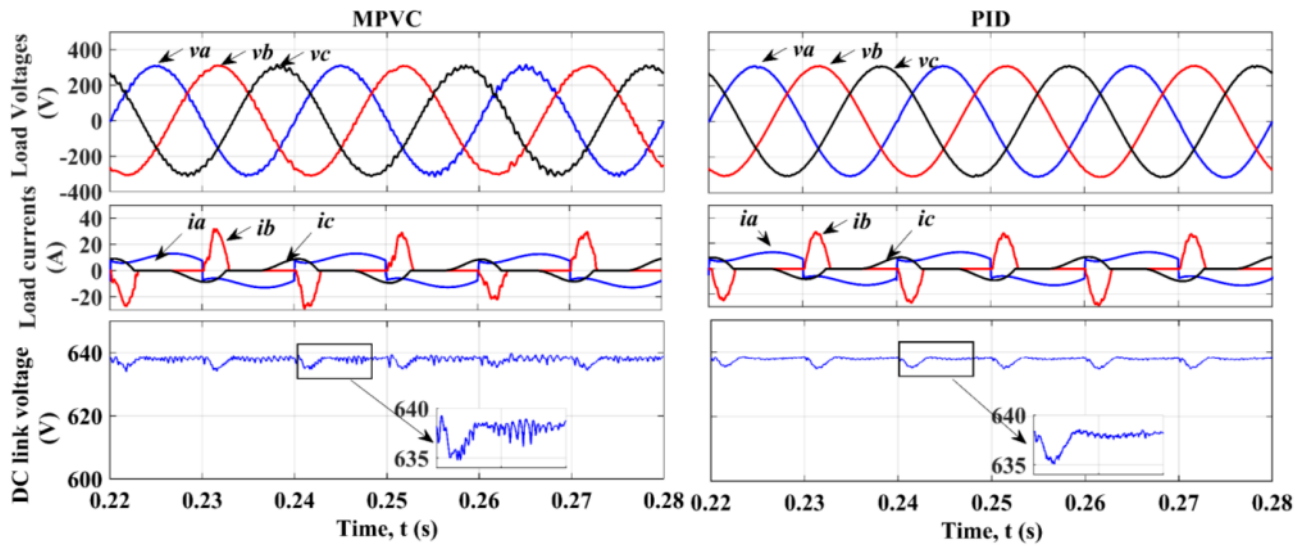


Figure 2.14. Simulation results of the SPS (Case Study 5: unbalanced non-linear loads) using (a) MPVC and (b) PID

Table 2.4 Comparative analysis of control with MPVC and PID algorithms

Experi ments	MPVC						PID					
	f_s (Hz)	% ΔV_{dc}	% THD			% VIF	f_s (Hz)	% ΔV_{dc}	% THD			% VIF
			Φ_a	Φ_b	Φ_c				Φ_a	Φ_b	Φ_c	
1	3754	0.3248	1.01	1.01	1.01	0.2248	4000	0.2004	1.29	1.3	1.26	0.1815
2	2071	0.6160	3.2	3.2	3.2	0.9592	4000	0.1971	1.4	1.4	1.4	0.1524
3	3968	1.7164	0.76	0.96	0.96	0.2007	4000	1.5411	1.45	1.47	1.44	0.1218
4	2177	1.6084	3.74	3.36	3.74	1.8977	4000	1.0109	1.49	1.48	1.45	0.3219
5	2436	0.8668	2.13	2.06	2.35	0.9426	4000	0.7095	1.62	1.5	1.54	0.0575

The results of the studies show that MPVC, like PID, is capable of regulating the load voltage with low harmonic distortion for both balanced and unbalanced resistive loads. Compared to PID control, MPVC provides lower harmonic distortion under active load conditions; a total harmonic distortion (% THD) below 1%.

The % THD with MPVC is higher in the case of inductive and nonlinear loads, but not more than 4%. This may be due to a delay in the change of inductive current, which reduces the accuracy of load voltage prediction.

MPVC provides higher voltage ripple (% ΔV_{dc}) in the AIV DC link compared to PID, but at higher power, MPVC provides a lower % ΔV_{dc} . This difference is evident compared to the dependencies shown in Fig. 2.17. According to IEEE standards, voltage

imbalance should be kept low at least 2% for sensitive loads. The value of the Voltage Imbalance Factor (VIF) is kept below 2% in all tested conditions for both control strategies. Additionally, the Voltage Imbalance Factor (VIF) is lower with MPVC than with PWM, in all load conditions, except in the case of a nonlinear load.

A particular feature of MPVC is that this algorithm operates with a variable switching frequency (f_s). The switching frequency is limited by the sampling time, as shown in the results. The switching frequency is capped at 5500 Hz in all case studies. Figure 2.18 shows the dependence of the MPVC switching frequency on the load power modification function and the power factor. The switching frequency increases significantly as the power factor increases and is limited to 5500 Hz.

2.4 Dynamic Mode of SPS Operation

To study the behavior of SPS in dynamic operation mode, a step-by-step change of the balanced resistive load from idle to the value ($R_a = R_b = R_c = 10 \Omega$) was performed in 0.2 seconds. The load voltages and currents for MPVC and PID algorithms are presented in Fig. 2.15, which further shows an enlarged view of the measured voltage with its reference time waveform at this change. The results show that the MPVC algorithm provides a faster dynamic response compared to the PID algorithm. The fast dynamic response of MPVC is possible to eliminate the modulation step.

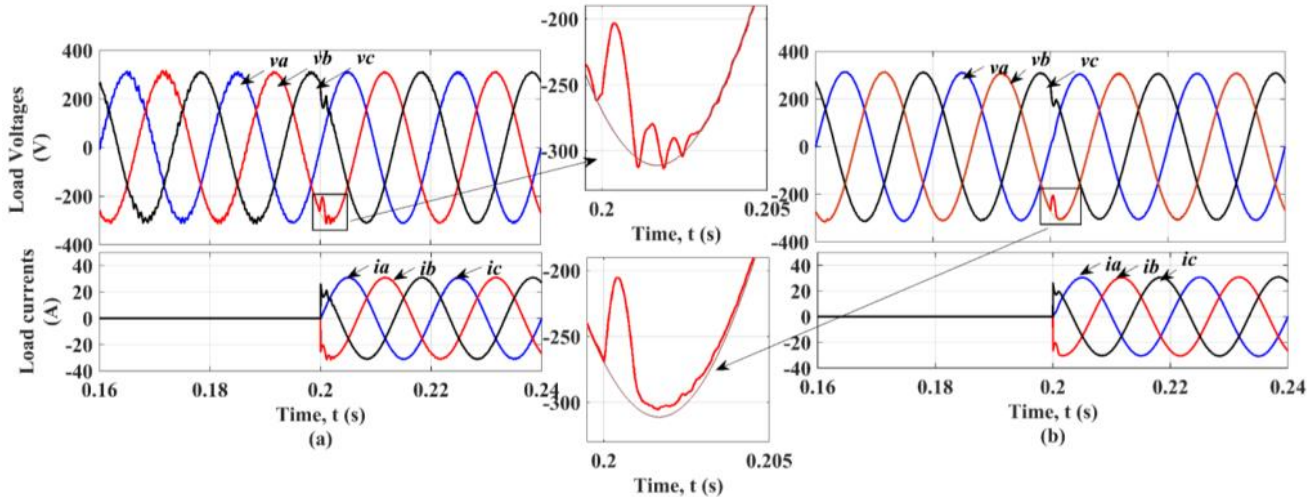


Figure 2.15. SPS load voltages and currents in dynamic mode for (a) MPVC- and (b) PID-algorithms

2.5 Control sensitivity analysis

Two tests were carried out to analyse the control sensitivity and asSPSs the impact of load change and changes in LC filter parameters on control characteristics in MPVC and PID-algorithms. The criteria for evaluating these tests are the average percentage of THD, % ΔV_{dc} and fs. In one load change resistance test, the active load power varies from zero to 80 kW at different power factors.

For the second test, the inductance of the filter varies from 1.5 to 3.5 mH with a change step of 0.2 mH, and the filter capacity from 50 to 100 μF with a change step of 5 μF . It can be noted that the load parameters in the proposed predictive model are not taken into account, while the standard load resistance is taken into account in the design of the PID regulator, which is ($R_L = 10 \text{ Ohm}$, $L_L = 1 \text{ mH}$). In addition, the model and the PID regulator "recognise" the standard values of the LC filter parameters, which are 2.5 mGh and 80 μF .

In Fig. 2.16 shows the change in THD from the change in load power and power factor for MPVC and PID. The deviation of THD from idling to high load in the MPVC algorithm is lower than in the PID algorithm at different power factors. It can be seen that MPVC has greater resistance to load changes than PID

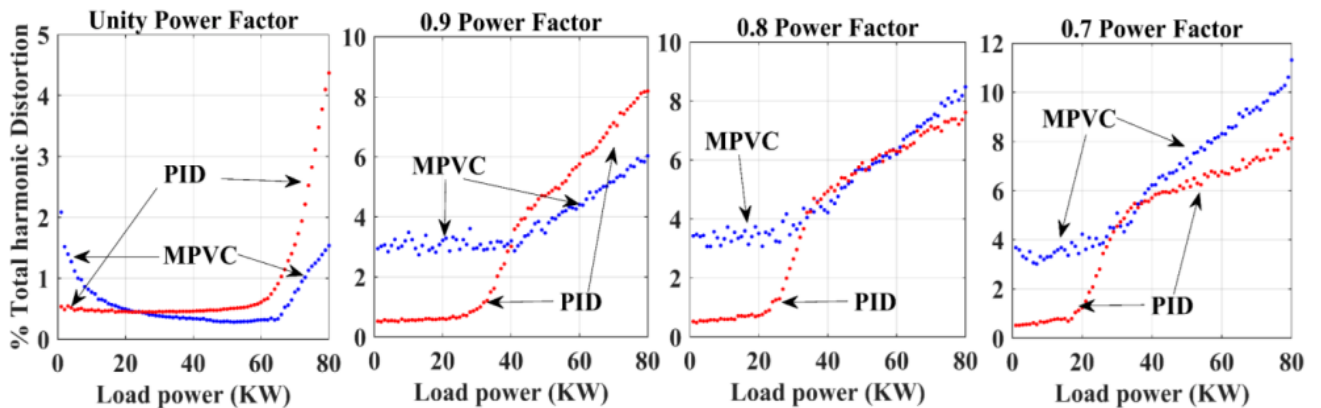


Figure 2.16. Change in % THD with change in load power at power factor equal to (a) 1, (b) 0.9, (c) 0.8, (g) 0.7

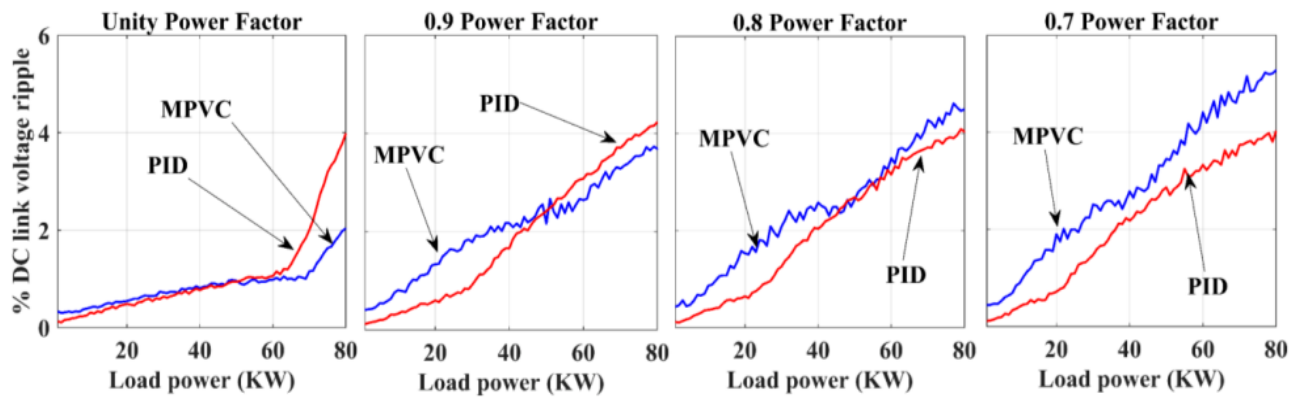


Figure 2.17. Change % ΔV_{dc} with change in load power at power factor equals to (a) 1, (b) 0.9, (v) 0.8, (g) 0.7

Changing ΔV_{dc} to control MPVC and PID when changing the load is shown in Fig. 2.17. Load change slightly affects the value of ΔV_{dc} for two control methods.

A high f_s value leads to large los_{SPS} of inverter switching and key overheating. In addition, the high variation of f_s complicates the design and selection of the LC filter. However, the MPVC works with a variable f_s that is limited by the sampling time and does not exceed the value of 5500 Hz for resistive and inductive loads. In Fig. 2.18 shows a change in f_s with a change in load power and power factor. In the case of a resistive load state, when the load increaSPS, f_s increaSPS sharply, but is limited to a value of 5500 Hz. The f_s value is limited by the sampling rate, as the control algorithm repeats during the sampling period.

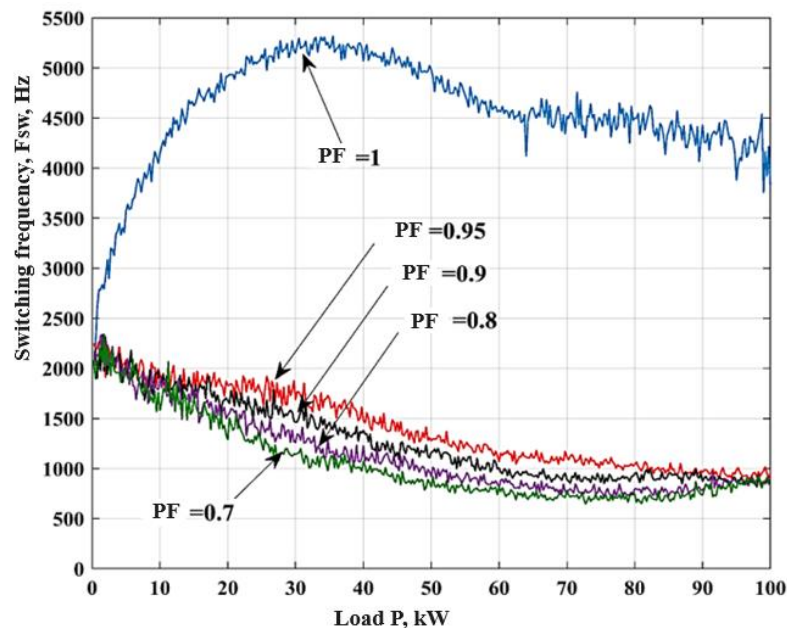


Figure 2.18. MPVC switching frequency with change in load power and power factor

Since control with the predictive model mainly depends on the parameters of the LC filter, two working conditions are considered in the LC filter change resistance test:

- ZP: change filter parameters until the system model has changed. In this case, the discrepancy between the actual parameters and parameters of the model is presented;
- SPS: change of filter parameters and, accordingly, simultaneous change of the system model.

2.6 Conclusions to the section

The studies carried out in section 2 allow you to more deeply and visually present electromagnetic process SPS and modes of operation of SPS with zero wire in the implementation of control algorithms based on PID and PR regulators and forecast model (MPVC). Based on the studies conducted:

In the Matlab Simulink package, a simulation model of SPS was developed when controlling AIV with zero wire based on three control methods: with PR regulator, PID regulator and with forecast model (MPVC);

A comparison of the functioning of the SPS with the zero wire was carried out when implementing the PR regulator and the PID regulator in static and dynamic modes.

A comparison of the functioning of SPS with zero wire was carried out when implementing a PID regulator and MPVC in static and dynamic modes under different natures of loads, including non-linear ones. It is shown that the MPVC-algorithm provides a faster dynamic response compared to the PID-algorithm. The results of the studies show that the MPVC, like the PID-algorithm, is able to regulate the load voltage with low harmonic distortion for a balanced and unbalanced resistive (including nonlinear) load. Compared to PID regulation, MPVC provides lower harmonic distortion in active load conditions below 1%.

3. CALCULATION SECTION

3.1 Optimisation of the MPVC algorithm

The implementation of the MPVC algorithm presented in the work is effective only if it is consistent with the development of emergency modes of the SPS, first of all the load mode at the output current up to a short circuit (CC) of the load. The task of extending the MPVC algorithm to emergency modes of operation of the SPS is complicated by the fact that in real conditions, loads or SC can occur in different topologies of the SPS scheme: single-phase, two-phase or three-phase SC. The task of the proposed algorithm is to automatically rebuild depending on the mode of operation of the SPS, maintaining, as far as possible, the quality of the output voltage in the phaSPS of the inverter, effectively limiting short-circuit currents, without affecting the load voltage of serviceable phaSPS.

In practice, to solve the above task, the proposed algorithm should include multi-purpose optimisation with limitations and additional properties of the algorithm, which increase the time of calculating the algorithm and lead to a delay between the moment of measurement and the application of a new control solution. To compensate for this delay, the proposed algorithm uses a two-step forecasting time. To reduce the time of calculations in the proposed algorithm, intelligent optimisation is used by removing repeated calculations that do not affect its performance, and by separating the emergency mode algorithm from the main algorithm. The emergency mode algorithm is activated only in case of a short circuit, which leads to a reduction in the calculation time required for the MPVC algorithm.

When the T_s sampling time decreases, the MPVC algorithm shows the best performance. To reduce T_s , high-speed microcontrollers must perform a large number of calculations in less time, resulting in a high cost. In this dissertation work, the proposed MPVC is optimised in such a way that it is divided into two algorithms: the normal mode algorithm and the emergency mode algorithm.

The purpose of the MPVC algorithm in normal mode is to control the output voltage of the inverter:

$$g = (v_a^* - v_a(k+2))^2 + (v_b^* - v_b(k+2))^2 + (v_c^* - v_c(k+2))^2 + F_{vlim} \quad (3.1)$$

Some voltage prediction calculations do not need to be performed at each switching state. To optimise time, voltage forecasting can be rewritten as:

$$\mathbf{v}(k+2) = \begin{bmatrix} v_a(k+2) \\ v_b(k+2) \\ v_c(k+2) \end{bmatrix} = \mathbf{Q}_v + j_1 \mathbf{e} \quad (3.2)$$

Where:

$$\mathbf{Q}_v = \begin{bmatrix} Q_{va} \\ Q_{vb} \\ Q_{vc} \end{bmatrix} = q_1 \mathbf{v}(k+1) + q_2 \mathbf{i}(k+1) + j_2 \mathbf{i}_L(k+1) \quad (3.3)$$

\mathbf{Q}_v is calculated only once for each interval.

In the algorithm of the SC mode, the target function is a combination between voltage and current regulation depending on the location and type of SC. For example, if a single-phase short circuit occurs in phase A, the control algorithm will act as a current regulator for phase A and a voltage regulator for other phaSPS, etc. Forecasting the current of the inverter in this algorithm is carried out using (4.5) with modifications:

$$\mathbf{i}(k+2) = \begin{bmatrix} i_a(k+2) \\ i_b(k+2) \\ i_c(k+2) \end{bmatrix} = \mathbf{Q}_i + j_3 \mathbf{e} \quad (3.4)$$

Where:

$$\mathbf{Q}_i = \begin{bmatrix} Q_{ia} \\ Q_{ib} \\ Q_{ic} \end{bmatrix} = q_3 \mathbf{v}(k+1) + q_4 \mathbf{i}(k+1) + j_4 \mathbf{i}_L(k+1) \quad (3.5)$$

There is no need to predict the entire load voltage and all inverter currents for each sampling period. According to the type and location of short circuit (SC), Q_i and Q_v are estimated once in each sample period, according to Fig. 3.1, illustrating the block diagram of the proposed optimised MPVC algorithm.

This algorithm is executed by each phase $j = a, b$ and c . For further optimisation, the target function in the emergency mode algorithm is divided into three target members (g_a, g_b, g_c), one target member of each phase. Each

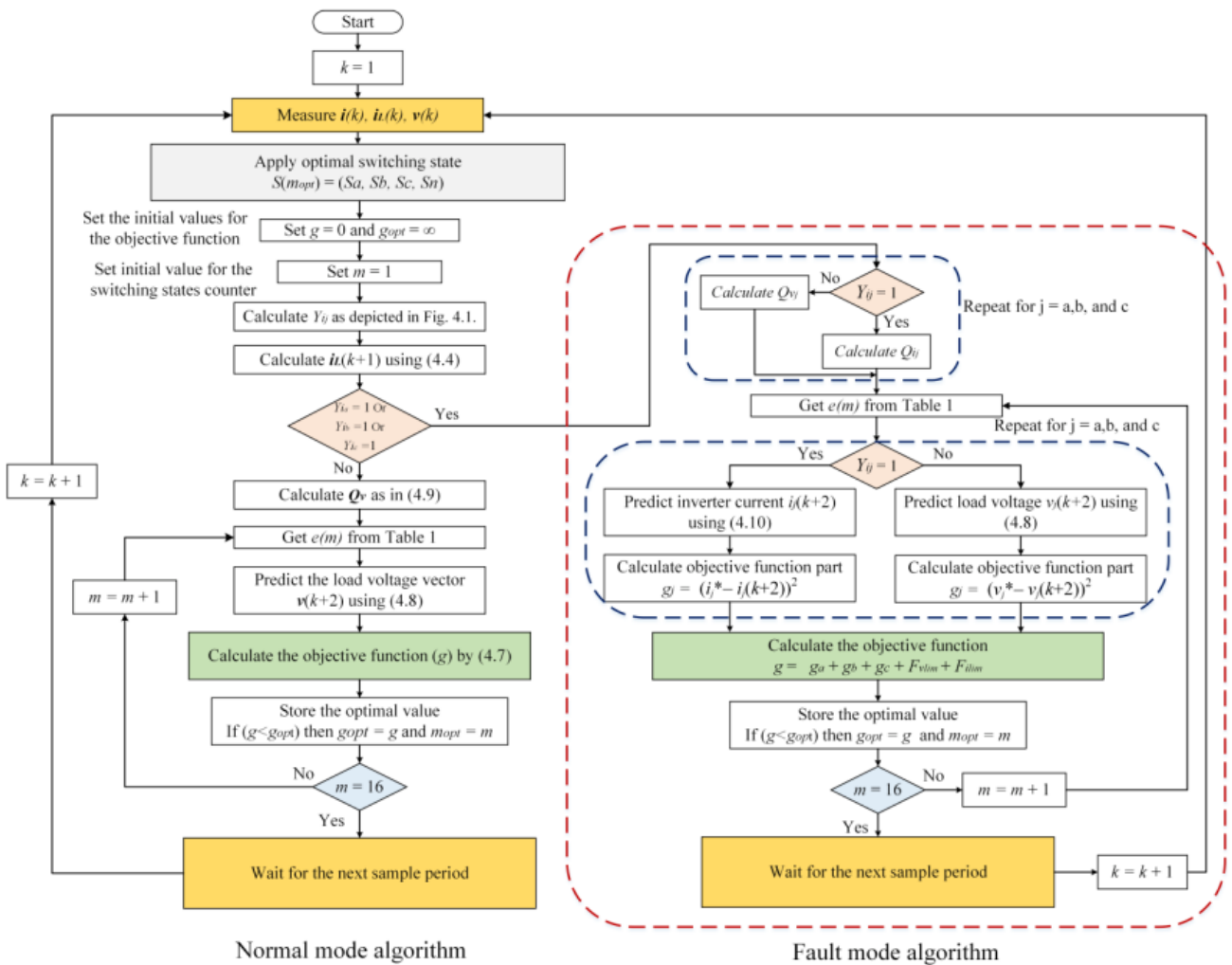


Figure 3.1. Flowchart of the optimised proposed MPVC algorithm

3.2 Experimental results of simulations of control methods

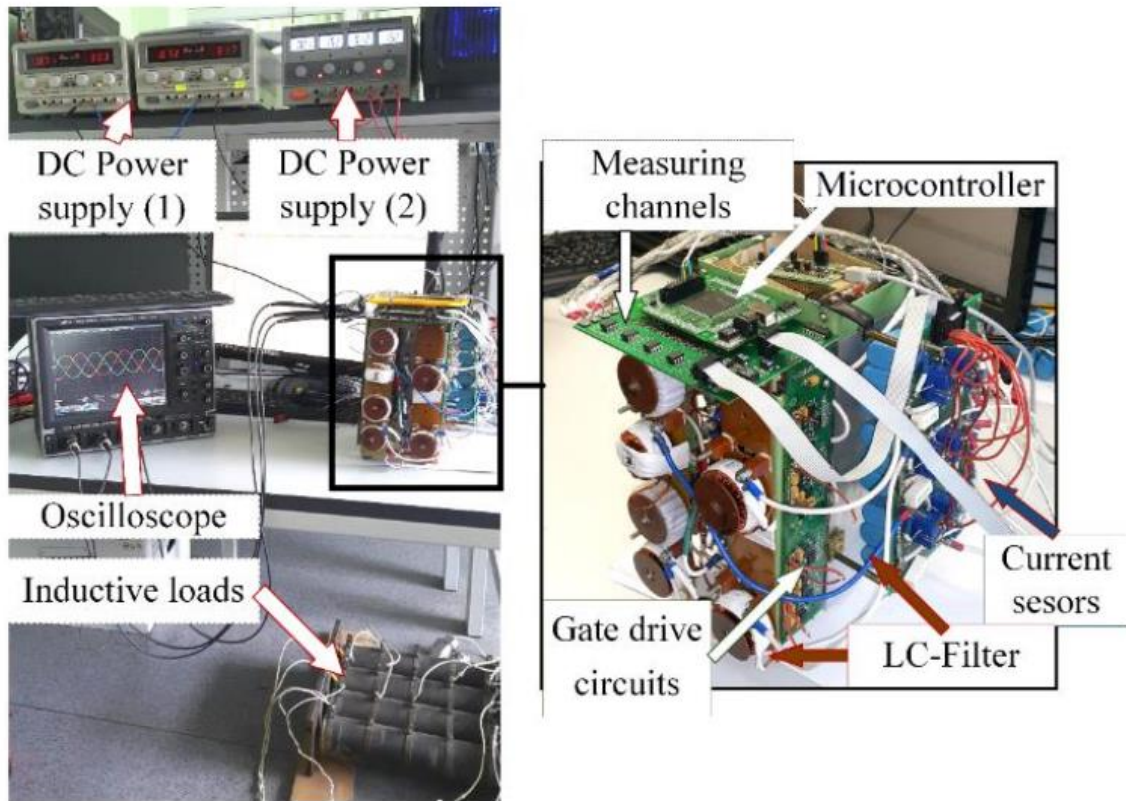
This unit presents the results of the experimental verification of the proposed MPVC algorithms. The testing scheme in practical experiments was used the same as in the modelling scheme. The microprocessor inverter control system is built taking into account the STM32F769BIT6 (216 MHz) microcontroller. Task signals are calculated

and recorded in the memory of the microcontroller. The LEM GAS 25-NP sensor is used as a current sensor in feedback channels. Measurements are made from nine analogue channels containing low-pass filters based on operational amplifiers. For safety reasons, the DC link voltage was selected at 60 V and was formed by two 30 V constant voltage sources included in series. Voltage feedback signals were measured directly without using a voltage sensor. An analog-to-digital converter is built into the microcontroller chip. The control signals produced by the microcontroller were supplied to the power transistor drivers (MOSFET IXFN110N60P3). The LeCroy Wave Runner oscilloscope was used to measure electrical quantities. A separate power supply was used to power the circuit of the microprocessor module and current sensors. The system parameters are given in Table 3.1. Pictures of the system and electrical diagram are shown in Fig. 3.2 A separate power supply was used to power the circuit of the microprocessor module and current sensors. The system parameters are given in Table 3.1. Pictures of the system and electrical diagram are shown in Fig. 3.2. A separate power supply was used to power the circuit of the microprocessor module and current sensors. The system parameters are given in Table 3.1. Pictures of the system and electrical diagram are shown in Fig. 3.2.

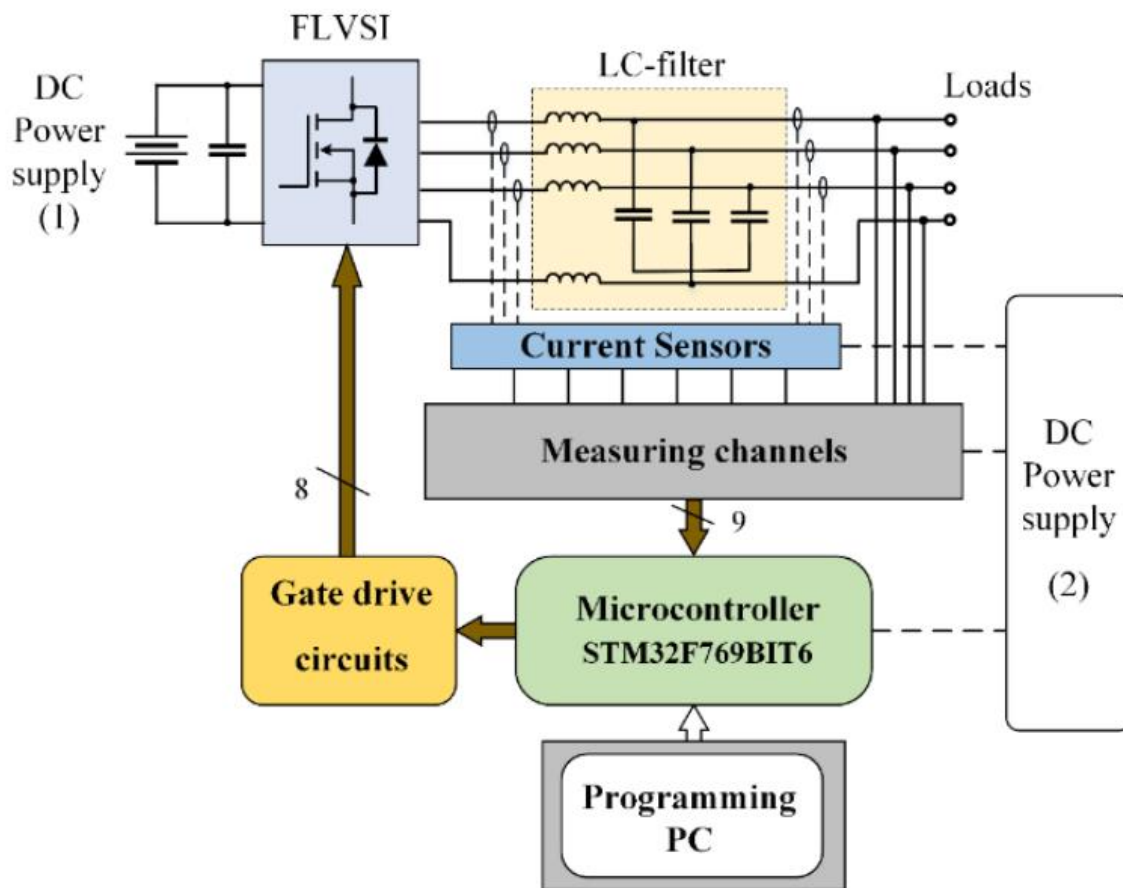
Due to the optimisation of the time performed for the proposed MPVC algorithm, the achieved calculation time of the proposed algorithm is 134 mx for the normal mode algorithm and 185 μ s for the emergency mode algorithm. For the microprocessor available in the laboratory, the sampling period for the normal mode algorithm is selected equal to 25 μ s, and the emergency mode algorithm is 32 μ s.

Table 3.1. Parmetres of the system

Parameter	Meaning
DC input power supply	$V_{dc}=60$ V, $P_{dc} = 720$ Watt
Sampling time	$T_s = 25\mu$ s / 32 μ s
DC-link capacitance	$C_{dc}=800$ μ F
LC filter	$R = 0.1$ Ω , $L = 1$ mH, $C = 90$ μ F



(a)



(b)

Figure 3.2. Experimental installation (a) and its functional scheme (b)

To evaluate the performance of the algorithm, testing was carried out in three modes: static mode of operation, transient process and short-circuit mode. Each of the operating modes was checked under different load parameters.

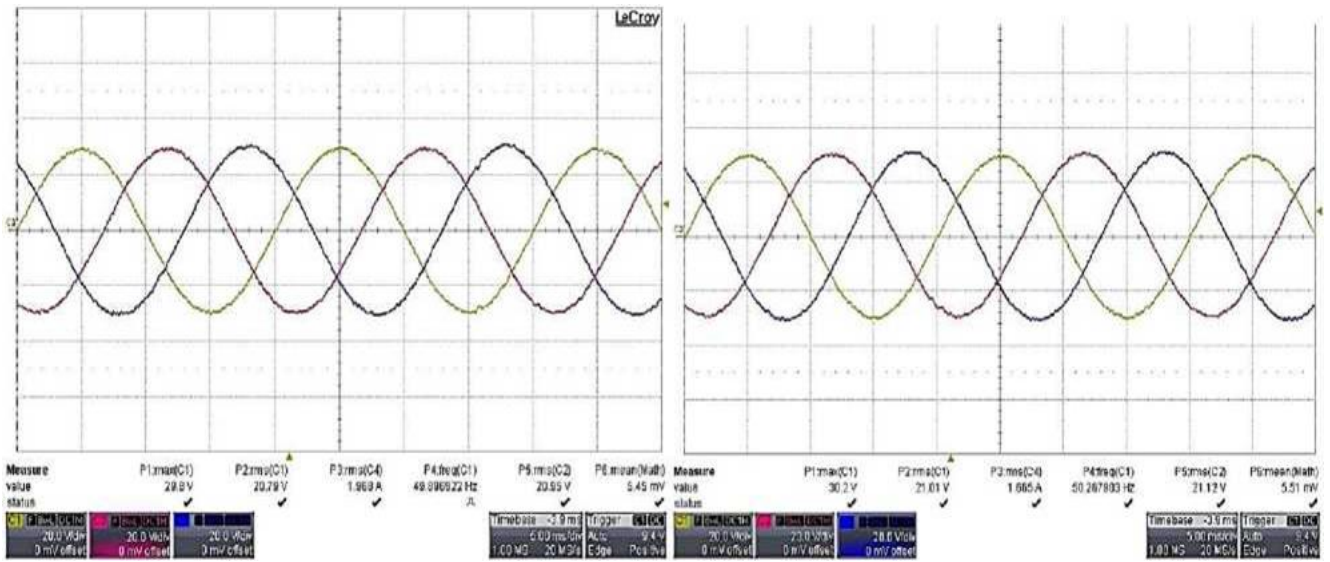
3.2.1 Static mode

The operation of the control algorithm in static mode was tested under different types of loads, presented in Table 3.2:

Table 3.2. - Parameters of load

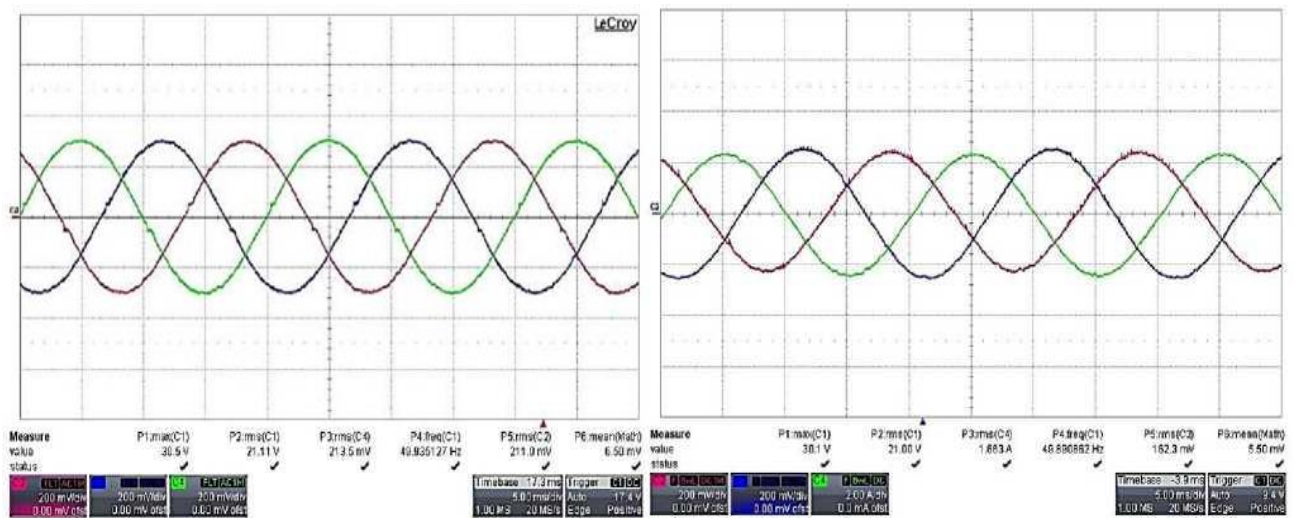
Experiment	Load parameters
1) Balanced Resistive Loads	$R_a = R_b = R_c = 10 \Omega$
2) Balanced Inductive Loads	$R_a = R_b = R_c = 12 \Omega$ $L_a = L_b = L_c = 4 \text{ mG}$
3) Unbalanced Resistive Loads	$R_a = 5 \Omega, R_b = 10 \Omega, R_c = 15 \Omega$
4) Unbalanced Inductive Loads	$R_a = 6 \Omega, R_b = 9 \Omega, R_c = 12 \Omega$ $L_a = 2 \text{ mG}, L_b = 3 \text{ mG}, L_c = 4 \text{ mG}$
5) Unbalanced Nonlinear Loads	Experiment(a): $L_f = 1.3 \text{ mH}, C_f = 1400 \mu\text{F}, R_a = 10 \Omega,$ Experiment(b): $L_f = 13.5 \text{ mH}, C_f = 2800 \mu\text{F}, R_a = 10 \Omega$

Oscillograms of load voltage, load currents, and neutral wire current at balanced loads are shown in Figures 3.3a – 3.5a. The corresponding voltage and current waveforms for the inductive load are presented in Figures 3.3b – 3.5b. The results of the experiments show that the algorithm is able to regulate the voltage regardless of the type of load (resistive or inductive). In the case of an inductive load, it was not possible to achieve an ideal balance of currents under laboratory conditions, so the current of the neutral wire is not zero in this case. An electronic load was used as a resistive load, which made it possible to reduce asymmetry to a minimum.



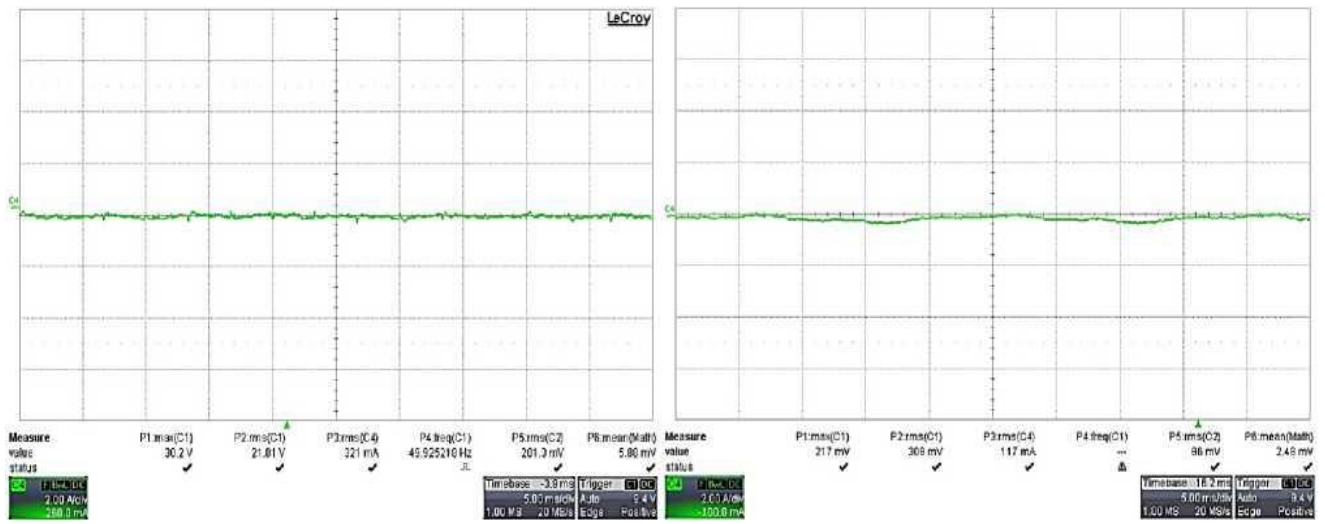
(a) (b)

Figure 3.3 - SPS load voltages at (a) balanced resistive loads and (b) balanced inductive loads



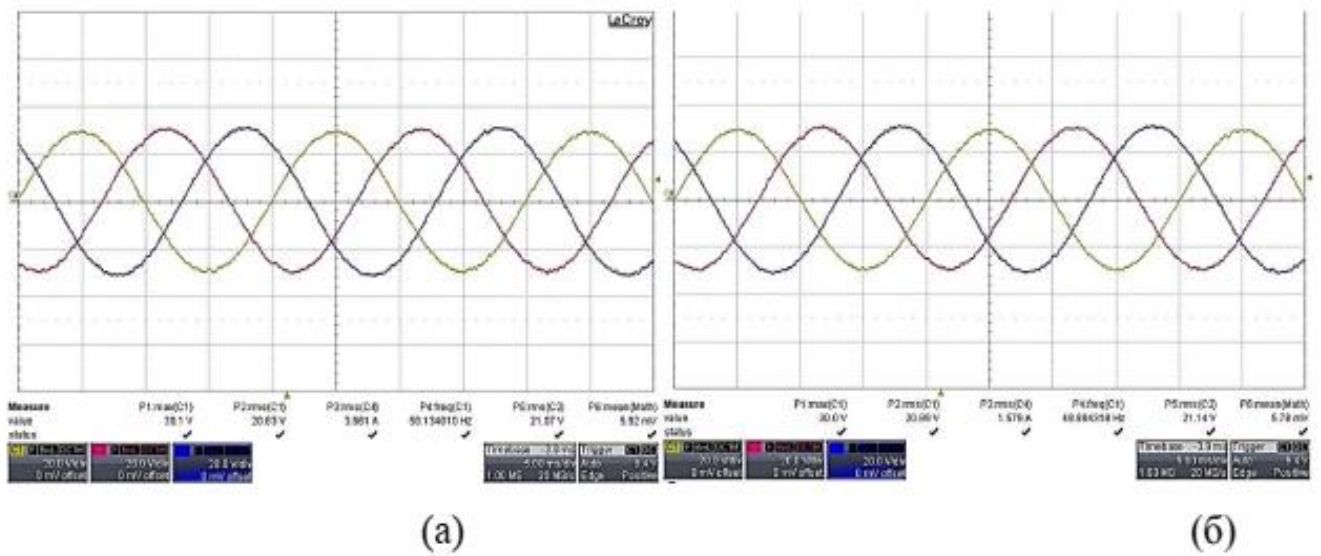
(a) (b)

Figure 3.4 - SPS load currents at (a) balanced resistive loads and (b) balanced inductive loads



(a) (b)

Figure 3.5 - SPS neutral wire current at (a) balanced resistive loads and (b) balanced inductive loads

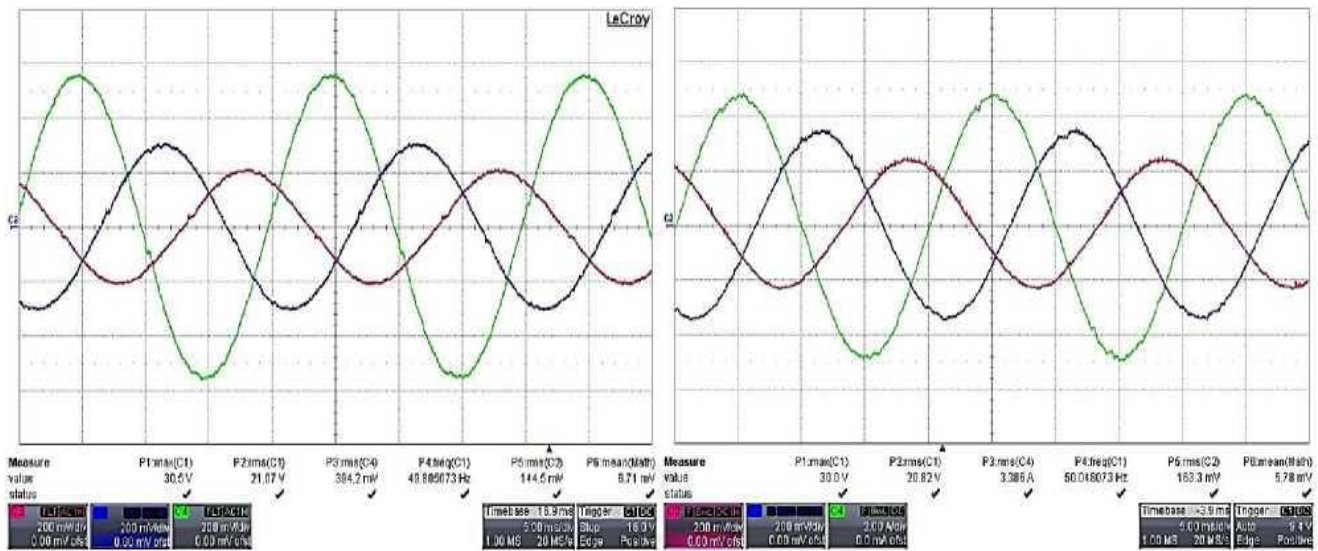


(a)

(b)

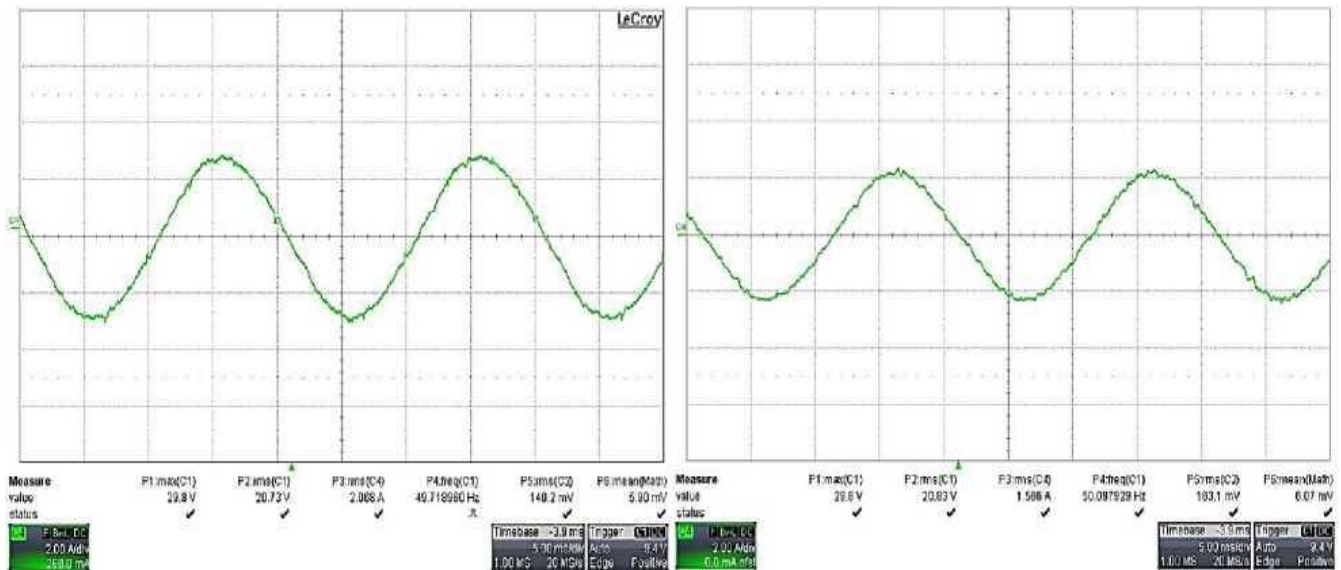
Figure 3.6 - SPS load voltage at (a) unbalanced resistive loads and (b) unbalanced inductive loads

In the case of an unbalanced load, the algorithm is able to control the voltage inverter so as to ensure a balanced load voltage (Fig. 3.6). Load voltages follow the reference voltages quite exactly, they are sinusoidal with a low harmonic distortion value. As shown in Fig. 3.7, the load currents are different and are determined by the impedance of the load of each individual phase, which causes the current flow in the neutral wire (Fig. 3.8).



(a) (b)

Figure 3.7 - SPS load currents at (a) unbalanced resistive loads and (b) unbalanced inductive loads



(a) (b)

Figure 3.8. SPS Neutral Current at (a) Unbalanced Resistive Loads and (b) Unbalanced Inductive Loads

To confirm the algorithm's performance under nonlinear loads, an experiment was conducted with the operation of a converter to a three-phase diode bridge with a resistive load and an LC filter. The load diagram is shown in Fig. 3.9.

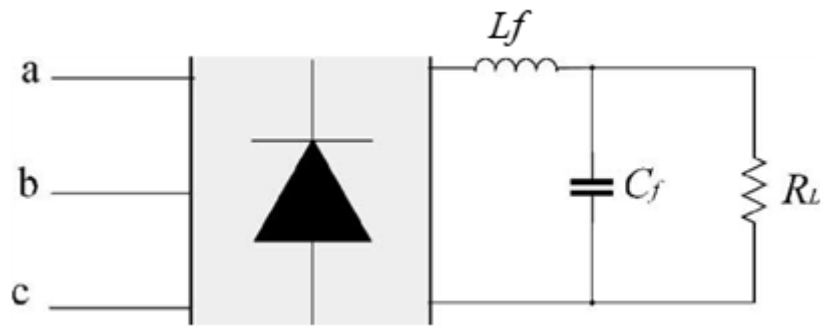
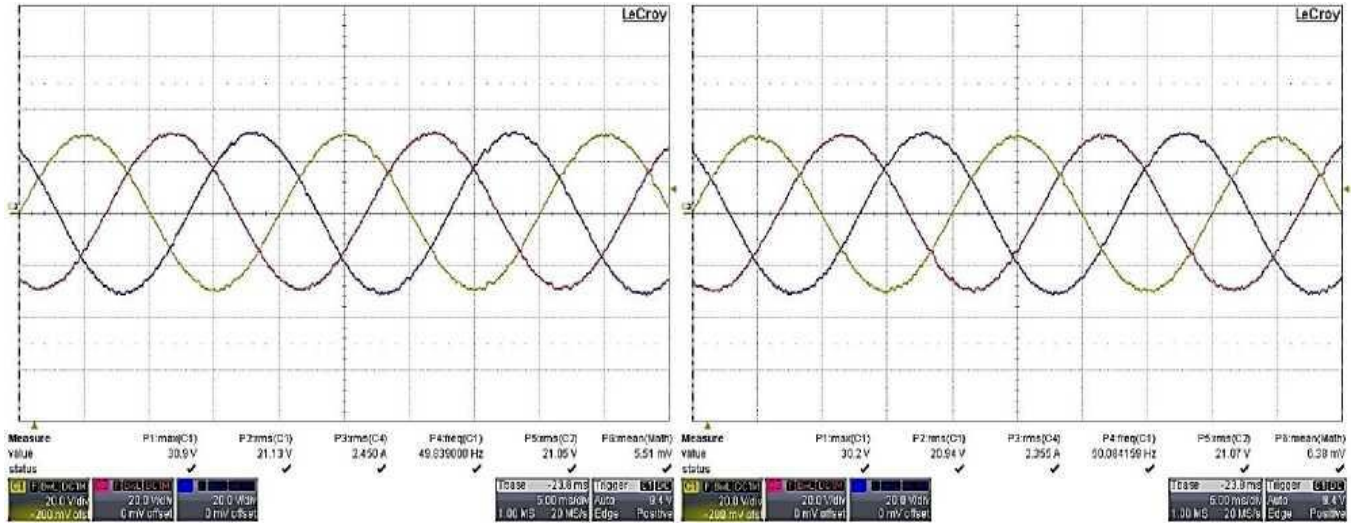


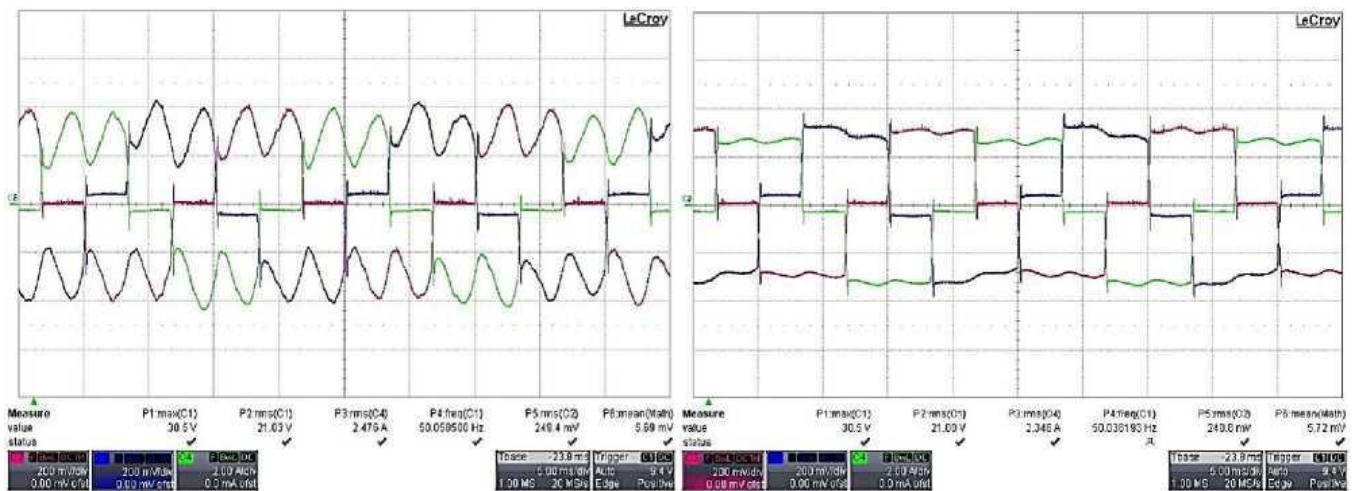
Figure 3.9 - Topology of nonlinear load of SPS used in the experiment



(a) (b)

Figure 3.10 - SPS load voltages at nonlinear loads: experiment (a) and experiment

(b)



(a) (b)

Figure 3.11 - SPS load currents at nonlinear loads: experiment (a) and experiment

(b)

During the experiment, an LC filter with different parameters was used (Table 3.2). Waveforms of phase voltages and phase currents are shown in Fig. 3.10 and Fig. 3.11 respectively. Although the currents consumed by the load are of a non-sinusoidal form, the phase voltages continue to accurately track the reference stresses and remain sinusoidal with a low harmonic distortion value.

3.2.2 Dynamic Mode

For practical testing of the SPS operation in dynamic mode, a stepwise change in the load resistance from no-load to the following values was used: $R_a = R_b = R_c = 10 \text{ Ohm}$ 0.2 seconds after the converter start. Load voltages and currents are shown in Figures 3.12 and 3.13, respectively.

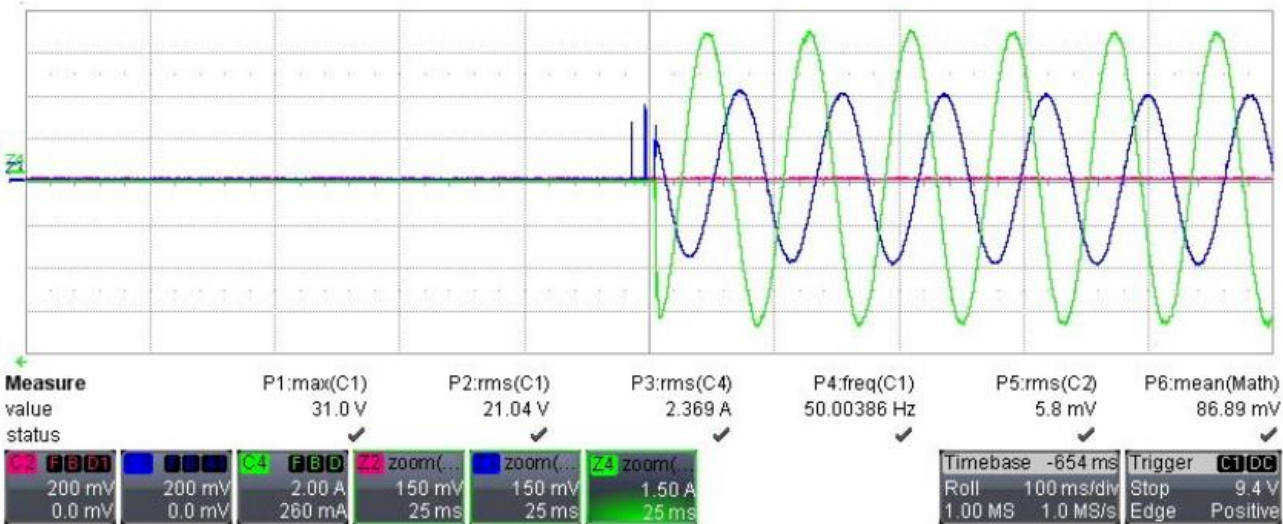


Figure 3.12 - SPS load currents in dynamic mode

The results of the experiment show that the amplitudes of the phase voltage remain unchanged after the load is connected. Moreover, the transient process ends in about 2 ms, which is an acceptable result. Phase voltage distortions are also at an acceptable level. As can be seen, during the transient process, turf is observed in the load current curves. However, this phenomenon does not affect the phase voltages, which follow the reference signals of the task exactly.

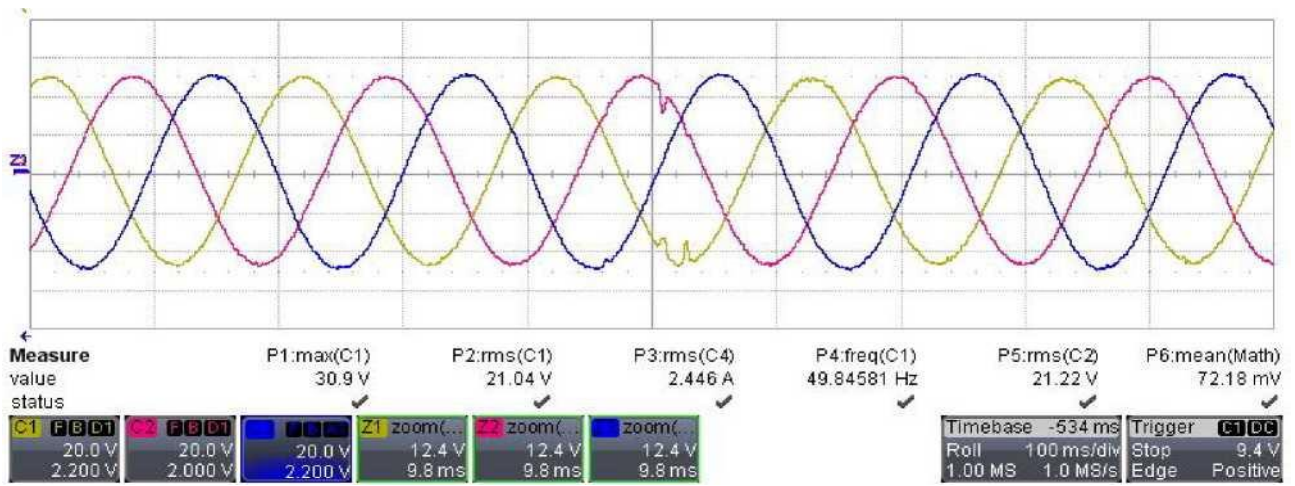


Figure 3.13 - Load voltage of SPS in dynamic mode

3.2.3 Emergency modes

In general, there are three types of emergency modes that can occur in any power supply system:

- 1- single-phase short circuit;
- 2- linear short circuit;
- 3- three-phase symmetrical short circuit.

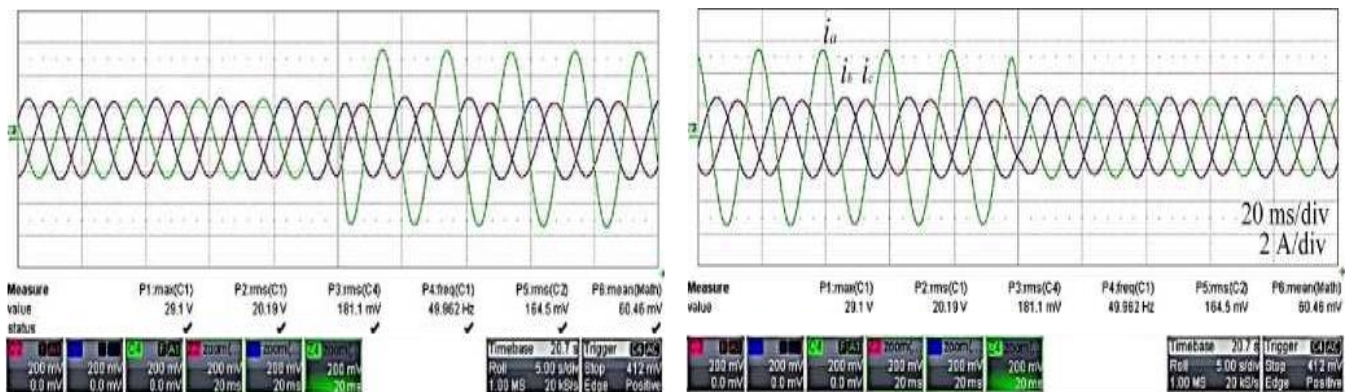


Figure 3.14 - Load current before a single-phase short circuit, during a single-phase short circuit and after.

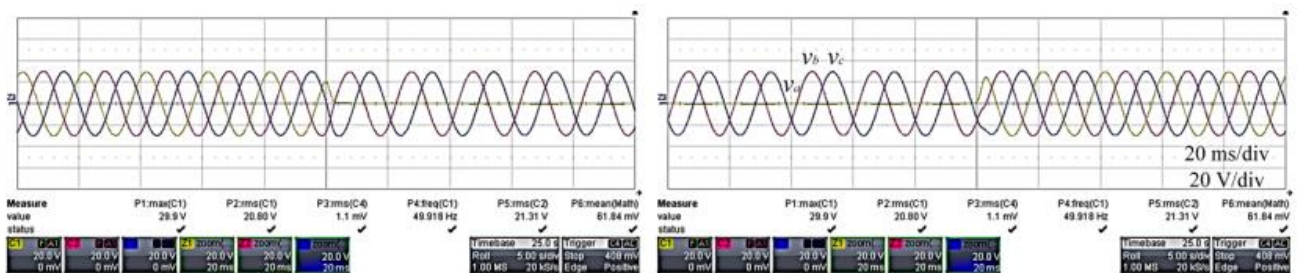


Figure 3.15 - Load voltage before a single-phase short circuit during a single-phase short circuit and after

The operation of the control algorithm has been tested experimentally on all types of emergency situations to show the efficiency of the algorithm and the possibility of limiting the current. A short circuit on the load side was carried out using an automatic contactor connected in parallel with the load for 1 to 3 seconds.

The load currents during a single-phase circuit in phase A are shown in Fig. 3.14. As can be seen from the waveform figure, the current in phase A is limited to 7 amperes and has a sinusoidal shape according to the reference signal of the current assignment, while the other phases operate independently in voltage regulation mode. As can be seen in Fig. 3.15 waveforms, a short circuit in phase A does not affect their operation in any way. After exiting the short-circuit state, the voltage in the phase returns to its normal state without overvoltages during the transient process.

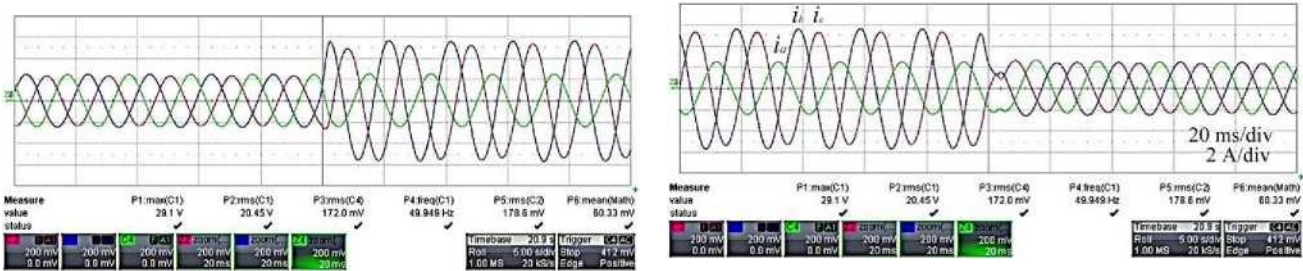


Figure 3.16 - Load current before a two-phase short circuit, during a two-phase short circuit and after

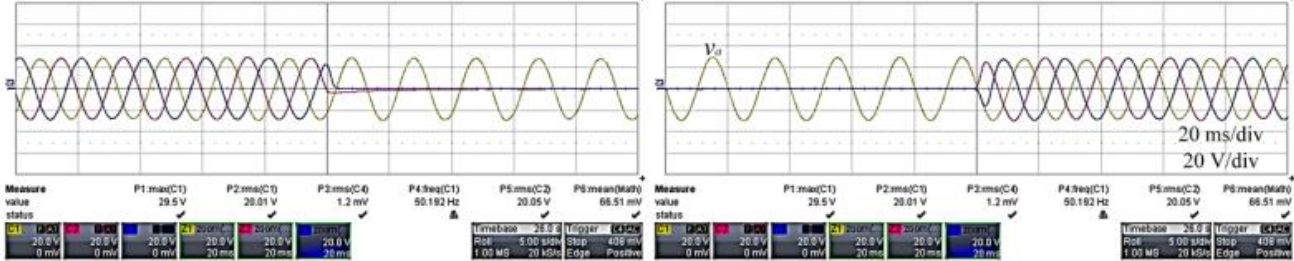


Figure 3.17 - Load voltage before a two-phase short circuit, during a two-phase short circuit and after

The developed control algorithm shows the same performance in the case of a two-phase short circuit, as shown in Figures 3.16 and 3.17. Currents in phases with short circuits are limited and have a sinusoidal shape according to the reference signal of the current assignment. The operation of the working phase is not disrupted. Single-phase and two-phase short-circuit modes are considered to be cases of unbalanced short circuit,

in which the algorithm allows you to effectively determine the phases in which an emergency occurred and change the control target to limit the load current, while maintaining the operability of the SPS in general and the operating phases in particular.

One of the most dangerous emergencies in three-phase solar power plants is a three-phase symmetrical circuit. The developed control algorithm allows you to effectively protect the power supply system from current surge by changing the purpose of voltage regulation control to current regulation. Fig. Figure 3.18 shows how the inverter, on the basis of which the SPS is built, generates a load of a given current in all phases during a short circuit. At the time when the SPS comes out of a short-circuit state, and at the time when the current is regulated, overvoltages may occur. Therefore, the algorithm, as in previous experiments, monitors the possibility of overvoltages and avoids inverter switching states that lead to voltages higher than the limit value. Such surge protection can lead to some voltage fluctuations when the inverter comes out of a short-circuit state, as shown in Fig. 3.19, which, however, are not critical.

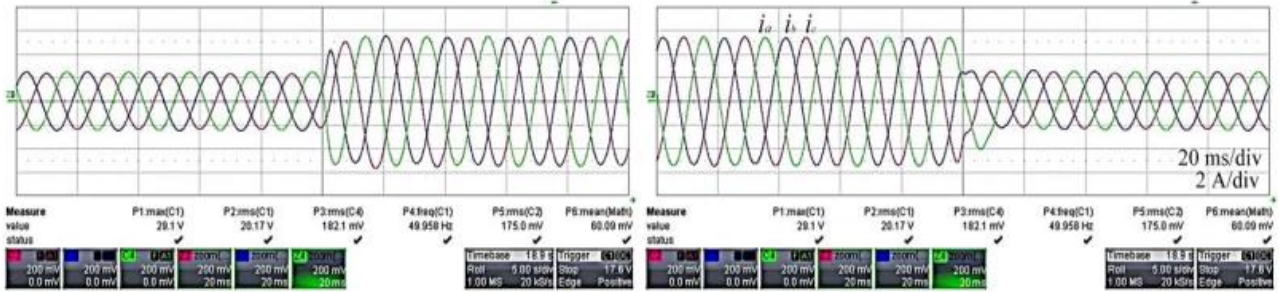


Figure 3.18 Load current before a three-phase short circuit, during a three-phase short circuit and after

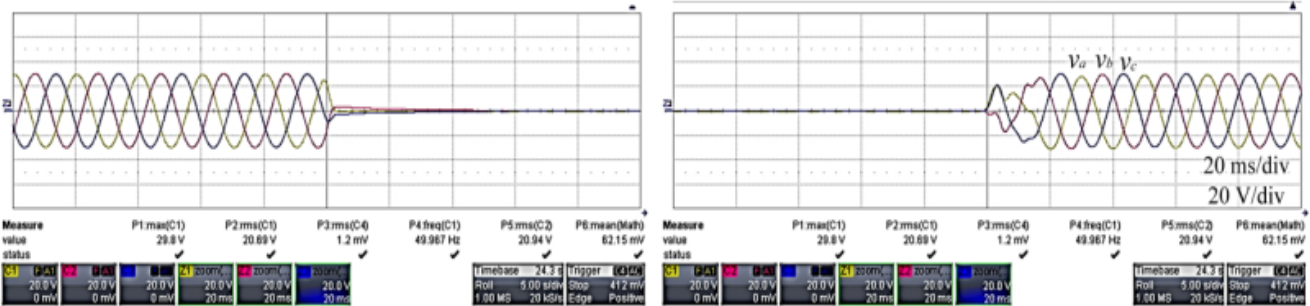


Figure 3.19. Load voltage before a three-phase short circuit, during a three-phase short circuit and after

3.3 Conclusions to the section

Studies conducted in Section 3 show that the predictive control algorithm (MPVC) is effective when using three-phase power supply systems implemented on the basis of a semiconductor converter (inverter). To check the theoretical provisions formulated in this work:

- 1) the MPVC algorithm was finalised for use in emergency modes of SPS operation;
- 2) a mock-up sample of a semiconductor SPS with a zero wire was made, on which physical experiments were carried out;
- 3) as a result of the experiments carried out, it is shown that the parameters of the output voltage of the SPS in terms of THD and dynamic response correspond to the results obtained during simulation modelling.

4 SAFETY OF LIFE AND BASICS OF LABOUR PROTECTION

4.1 Safety in the operation of electrical equipment and power grids

Maintenance of electrical equipment is allowed to persons at least 18 years old who do not have medical contraindications that interfere with the performance of work, received introductory and primary briefings at the workplace, production training, knowledge testing.

The electrician must know the scheme of power supply of production facilities, must have skills in techniques of technical methods of maintenance of electrical installations. It is provided with all personal protective equipment and overalls. Tools and defences must be tested, serviceable and used for their intended purpose [13].

When operating existing electrical installations, electrical protection means and safety devices are used. Manual switching on and off of equipment with a voltage of more than 1000 V must be performed in dielectric gloves, wheels or on a mat. Disconnections are performed as follows: disconnect disconnectors, remove fuse inserts, disconnect the network drive. After hanging the poster, check the absence of voltage on the disconnected section of the network. The operational journal makes a record of the outage. Inclusions are carried out only after the mark in the journal on the completion of work with the indication of the responsible person.

The security of execution is also ensured by organisational measures. These include the registration of work of outfits, registration of admission to work, supervision during the performance of work.

The outfit is a written work permit in electrical installations, which determines the place, time, beginning and end of work; the conditions of its safe

Carrying out, the composition of the brigade and persons responsible for safety. Without order by oral or written order, but with a mandatory entry in the journal, such works as cleaning the premiSPS to the fencing of electrical equipment, cleaning casingsings, adding oil to bearings, caring for collectors, contact rings, brushes, replacing fuSPS can be performed. When working with electrical installations with a voltage of up to 1000 V without relieving voltage, it is necessary: to protect other voltage-enerated parts located near the workplace, to which accidental touch is possible; work in dielectric

galoshes or standing on an insulating stand, or on a dielectric carpet; use a tool with insulating handles (in screwdrivers, in addition, a rod must be isolated), in the absence of such a tool, use dielectric gloves.

When performing work without de-energizing on current-conducting parts with the help of insulating protective equipment, it is necessary to: keep the insulating parts of the protection equipment by the handle to the limiting ring; place the insulating parts of the protective equipment so that there is no danger of overlapping on the surface of the insulation between the current-carrying parts of the two phaSPS or locking on the ground; use only dry and clean insulating parts of protective equipment with intact lacquer coating.

If a violation of the varnish coating or other malfunctions of the insulating parts of the protection products are detected, their use should be immediately discontinued.

Variable inspections of electrical equipment and networks should be carried out by another electrician. When inspecting, you should pay attention to the following: no changes in the state of electrical equipment during its operation; the degree of corrosion, painting of pipes, krZpilling elements; serviceability of wire and cable inputs into electrical equipment; serviceability of grounding devices; presence of warning posters and marking signs on explosive electrical equipment; presence of all bolts provided for by the design that krZPping shell elements (they must be well tightened); getting on electrical equipment of spray, drops and dust.

If abnormal operation of the power transformer is detected, the next electrician must remove it from work with the mandatory observance of all personal safety measures, using the necessary personal protective equipment. Such a shutdown is carried out with: strong uneven noise and crackling inside the transformer; abnormal and ever-increasing heating of the transformer at nominal load and operation of cooling devices; oil emission from the expander or rupture of the exhaust pipe diaphragm; oil leaks with a decrease in its level below the minimum allowable.

At the same time, an entry is made in the operational journal and reported to the person responsible for the electrical economy.

The rules for the technical operation of consumer electrical installations and safety rules for the operation of consumer electrical installations require regular inspections and repair of electrical networks, as well as measurement of resistance and insulation.

4.2 Study of the sustainability of work in emergencies of enterpriSPS of the electrical and lighting industry

The stability of the work of electrical and lighting industry facilities is understood as its ability in an emergency to produce products in the planned volume and nomenclature, and when receiving medium destruction or breaking ties with cooperation and supplies, resume production in the shortest possible time.

Under the stability of the work of objects that do not directly produce material values, they understand their ability to perform their functions in emergency conditions.

The following factors affect the stability of the operation of the facilities of the electrical and lighting industry in emergency conditions:

- reliability of protection of workers and employees;
- the ability of the engineering and technical complex of the facility to resist to a certain degree of damaging factors of natural disaster, accidents, disasters and modern weapons;
- protection of the object from secondary damaging factors (fires, explosions, infection with toxic substances);
- reliability of the system for providing the object with everything necessary for production (raw materials, fuel, components and parts, electricity, water, gas, etc.);
- stability and continuity of production management and CA;
- preparedness of the facility for the conduct of RIN and work on the disrupted production.

Protection of workers and employees is achieved in four main ways:

- shelter of people in Defence structures;
- carrying out evacuation measures;
- radiation and chemical protection;
- medical and biological protection.

Reliable protection of the production personnel of the facility is possible only with the complex use of all major methods of protection.

The protection of production assets is to increase the opposition of buildings, structures and structure of the facility to damaging factors and protection of technological

equipment, machine tools, systems and communications and other means that form the basis of the production process.

Creation of reliable systems of electrical, water and heat supply of objects:

A) increasing the stability of electricity supply:

- distribution of the power grid scheme into independently working parts;
- ringing power grids and connecting them to several sources of energy supply;
- creation of a reserve of diesel power plants;

B) increasing the stability of water supply systems:

- water supply from two independent sources, one of which is underground;
- protection of water sources and clean water tanks;
- creation of bypass (bypass) lines around water towers;

C) increasing the stability of gas, heat and fuel supply systems:

- distributed gas pipelines should be made underground and provide for their ringing;
- gas distribution stations and strong points of bypass gas pipelines are provided in the underground version;
- install automatic shutdown devices at the main nodal points of the systems, which are triggered in case of accidents.

Increased fire resistance:

- maximum reduction of fuel reserves and explosive substances;
- carrying out preventive fire-fighting measures;
- preparation of fire extinguishing forces and means.

Creating the stability of the material and technical supply system. At the facilities of the electrical and lighting industry, reserves of raw materials, fuel, components and parts, equipment are created that allow you to continue work in case of supply disorganisation.

Creating the stability of the control system:

- preparation of PU (protected);
- provision of PU means of communication;
- use of an automated control system. Preparation for accelerated (immediate) resumption of disrupted production;
- development of the necessary technical and technological documentation;

- creation of stocks of material resources for the establishment of works;
- Development of calculations of forces and means for restoration work;
- determination of the likely sequence of work to resume production, taking into account available resources and local conditions.

In addition, the stability of the work of enterpriSPS of the electrical and lighting industry will be influenced by the presence of a trained labour force.

Improving the reliability and efficiency of production management:

- creation of a stable communication system at the facility;
- high training of the management team;
- timely making the right decisions and setting tasks for subordinates in accordance with the current situation.

Increasing the stability of the work of the object of the electrical and lighting industry is achieved in advance of a complex of engineering, technical, technological and organisational measures that are aimed at minimising the impact of damaging factors and creating conditions for the elimination of the consequences of the emergency.

Engineering and technical measures are a set of works that increase the stability of production buildings and structures, equipment, utilities, systems.

Technological measures ensure an increase in the stability of the facility by changing the technological process, which contributes to the simplification of product production and eliminates the possibility of secondary damaging factors.

Organisational measures involve the development and planning of actions of the management command and command staff of the headquarters, services and the formation of the CO in the protection of workers and employees, the conduct of the RINR, the resumption of production.

GENERAL CONCLUSIONS

In the presented qualification work, the following conclusions can be drawn:

– a study of the modes of operation of a semiconductor three-phase SPS based on a semiconductor converter (inverter) was carried out, which implements the predictive control algorithm. The studies conducted showed the realisation, efficiency and prospects of using the above algorithm to achieve the necessary quality of the output voltage. As a result of the research done in the work.

– the features of the application and construction of autonomous semiconductor SPS when working on various types of loads and as part of autonomous networks, in particular, microgrid, have been studied and analysed.

– an algorithm for predictive control of the output voltage of AIV with a zero wire has been developed, which minimises the error between the output and reference voltage.

– The Matlab Simulink package has developed a simulation model of SPS when controlling an autonomous inverter with a zero wire based on three control methods: with a PR regulator, a PID regulator and with a predictive model.

– comparative studies of SPS with predictive control, functioning on the basis of algorithms of proportional-integral-differential (PID) and proportional-resonance (PR)-regulations, have been carried out.

– Algorithms for emergency protection of semiconductor SPS with predictive control of load current have been developed.

– To verify theoretical studies and conclusions, a mock-up sample of a semiconductor SPS with zero wire was produced, on which experiments were carried out.

LIST OF LINKS

1. Vaclav Smil, *Energy Transitions: History, Requirements, Prospects* (Santa Barbara, Calif.: Praeger, 2010), vii. For alternative definitions, see Benjamin K. Sovacool, «How Long Will It Take. Conceptualizing the Temporal Dynamics of Energy Transitions», *Energy Research & Social Science*, vol. 13, 2016, 202-203.
2. Smil, Vaclav. *Energy and Civilization: a History*. MIT Press, 2018. 4. <https://irena.org/newsroom/pressreleases/2018/Oct/Egypt-Could-Meet-Morethan-50-percent-of-its-Electricity-Demand-with-Renewable-Energy>.
3. Zamora R, Srivastava AK. Controls for microgrids with storage: Review, challenges, and research needs. *Renew Sustain Energy Rev* 2010.
4. Palizban O, Kauhaniemi K. Hierarchical control structure in microgrids with distributed generation: Island and grid-connected mode. *Renew Sustain Energy Rev* 2015.
5. Vandoorn TL, De Kooning JDM, Meersman B, Vandeveldel L. Review of primary control strategies for islanded microgrids with power-electronic interfaces. *Renew Sustain Energy Rev* 2013.
6. Rocabert J, Luna A, Blaabjerg F, Rodríguez P. Control of power converters in AC microgrids. *IEEE Trans Power Electron* 2012.
7. Liu X, Deng Y, Liu Q, He X, Tao Y. Voltage unbalance and harmonics compensation for islanded microgrid inverters. *IET Power Electron* 2014.
8. X. Wang, J. M. Guerrero, F. Blaabjerg, and Z. Chen, “A review of power electronics based microgrids,” *J. Power Electron.*, vol. 12, no. 1, pp. 181–192, 2012.
9. P. G. Arul, V. K. Ramachandaramurthy, and R. K. Rajkumar, “Control strategies for a hybrid renewable energy system: A review,” *Renew. Sustain. Energy Rev.*, vol. 42, pp. 597–608, 2015.
10. A. Mohd, E. Ortjohann, D. Morton, and O. Omari, “Review of control techniques for inverters parallel operation,” *Electr. Power Syst. Res.*, vol. 80, no. 12, pp. 1477–1487, 2010.
11. S. B. and B. Chowdhury, “Hybrid AC / DC Power Distribution Solution for Future Space Applications,” *Proc. IEEE PESGM*, vol. 65401, pp. 1–8, 2007.

12. Z. Jiang and X. Yu, "Hybrid DC- and AC-linked microgrids: Towards integration of distributed energy resources," 2008 IEEE Energy 2030 Conf. ENERGY 2008, 2008.
13. Z. Chen, J. M. Guerrero, F. Blaabjerg, and S. Member, "A Review of the State of the Art of Power Electronics for Wind Turbines," IEEE Trans. Power Electron., vol. 24, no. 8, pp. 1859–1875, 2009.
14. Peng Li, Bai Dan, Kang Yong, and Chen Jian, "Research on three-phase inverter with unbalanced load," in Nineteenth Annual IEEE Applied Power Electronics Conference and Exposition, 2004. APEC '04., 2004, vol. 1, no. C, pp. 128–133.
15. D. Soto, C. Edrington, S. Balathandayuthapani, and S. Ryster, "Voltage balancing of islanded microgrids using a time-domain technique," Electr. Power Syst. Res., vol. 84, no. 1, pp. 214–223, 2012.
16. P. K. Goel, B. Singh, S. S. Murthy, and N. Kishore, "Isolated wind-hydro hybrid system using cage generators and battery storage," IEEE Trans. Ind. Electron., vol. 58, no. 4, pp. 1141–1153, 2011.